CFEL Colloqium February 5th 2015

Stagnation layers at the collision front between counter-streaming plasma plumes: formation, properties and potential applications

John T. Costello

National Centre for Plasma Science & Technology (NCPST)/
School of Physical Sciences, Dublin City University

www.physics.dcu.ie/~jtc

Outline of the Talk

I. Colliding plasmas - some fundamentals

2. Colliding plasma – some motivations

3. Diagnostics – mapping plasmas in space-time

4. Key properties – potential applications

5. Summary and next steps

DCU Laser Plasma/Atomic Physics

Laser Plasma @ NCPST - 6 laboratory areas focussed on pulsed laser matter interactions (spectroscopy/ imaging)

Research Domains:

1. *Colliding Laser Produced Plasmas*
2. *Optical and Particle Diagnostics of Laser Produced Plasmas*
3. Laser Induced Breakdown Spectroscopy (LIBS) in the Vacuum-UV
4. Pulsed Laser Deposition (PLD) of Materials
5. Photoionization of Atoms and Ions with Laser Plasma and Free Electron Laser Light Sources

Some Current Projects:

1. *UV-Vis imaging, spectroscopy and interferometry of colliding laser produced plasmas [with and without laser reheating]*
2. Double Pulse VUV-LIBS for Elemental Characterisation in Steel
3. *Ion emission from single and colliding laser plasmas*
4. PLD of ZnO nanostructures
5. 2 photon and 2 colour photoionization of atoms with EUV FEL

Part I – Single & Colliding Plasma Basics

Laser Pulse 1064 nm/
0.01 - 1 J/ 150ps-10 ns

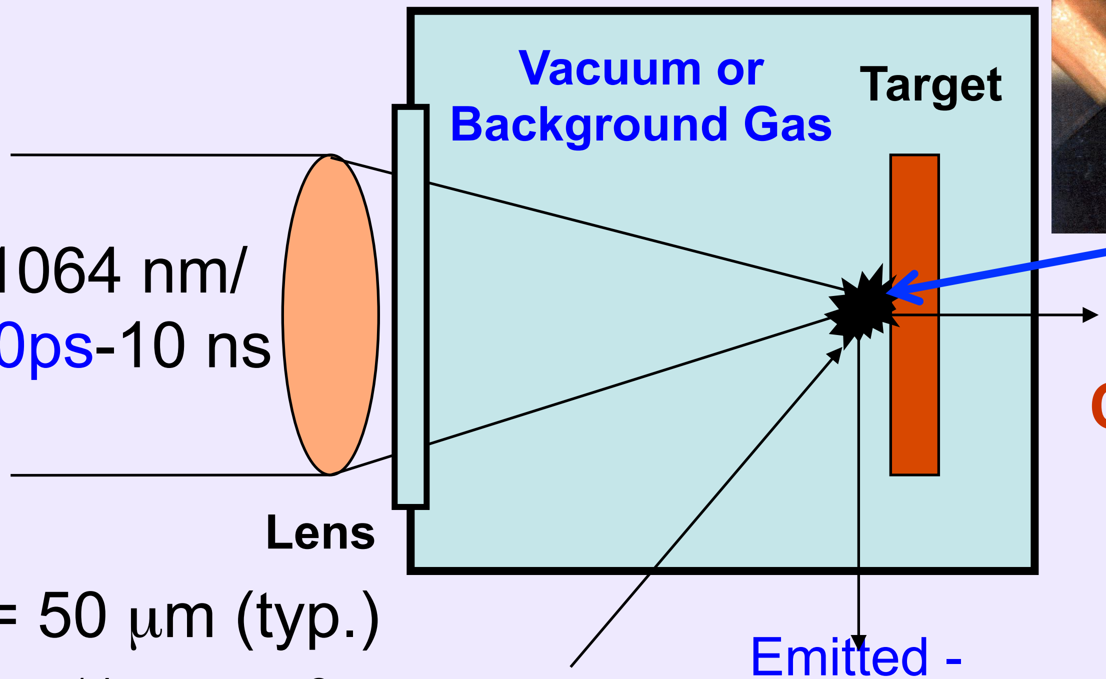

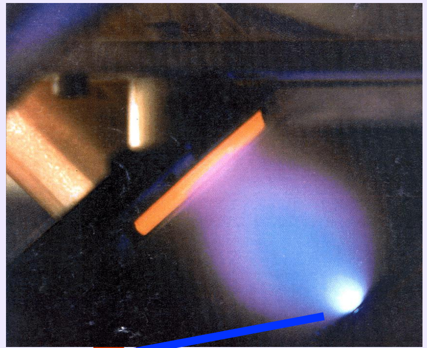

Plasma Assisted Chemistry

Spot Size = 50 μm (typ.)

Φ: 10^{11} - 10^{14} W.cm^{-2}

T_e : 10 - 500 eV

N_e: 10^{21} cm^{-3}

$V_{expansion} \geq 10^6$ cm.s^{-1}

Emitted -
Atoms,
Ions,
Electrons,
Clusters,
IR - X-ray Radiation

Part I – Single & Colliding Plasma Basics

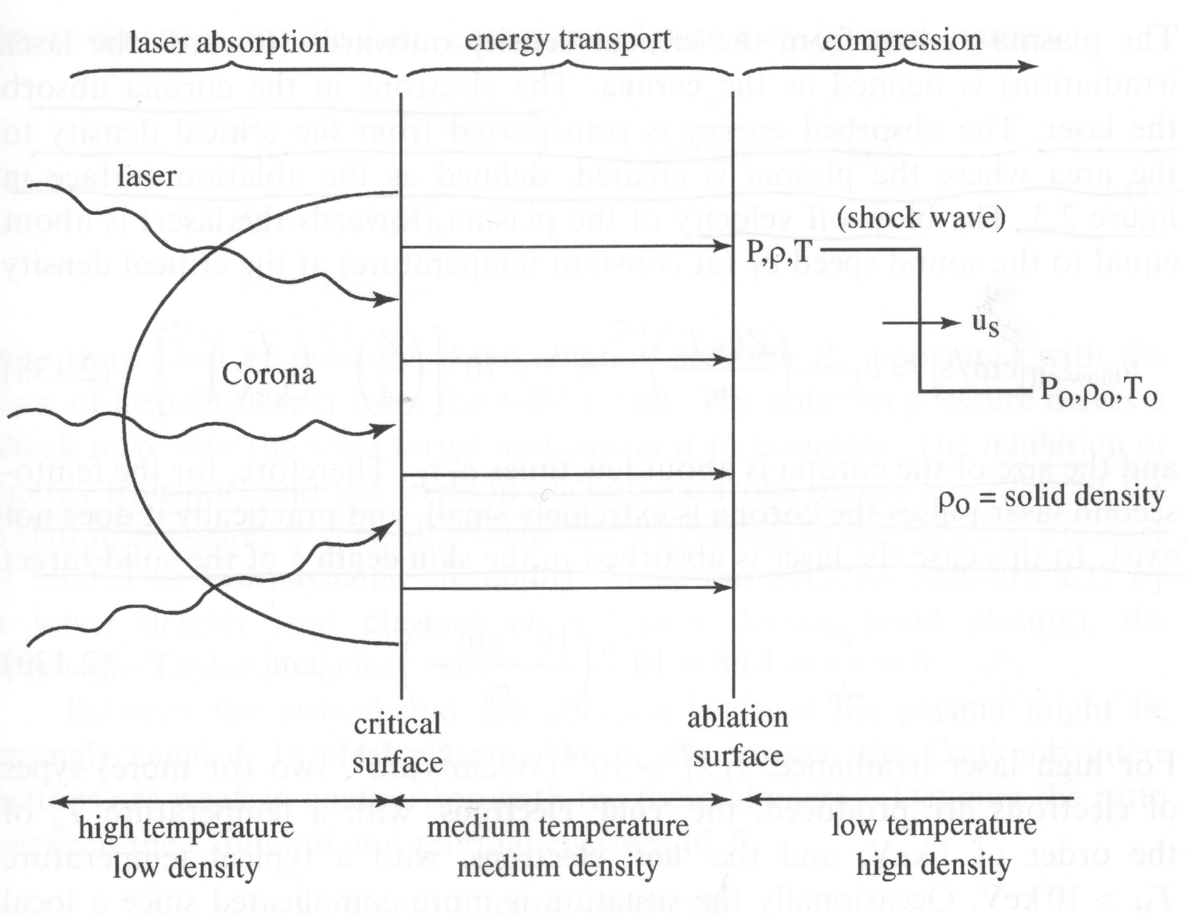

Figure 2.3. A schematic description of laser–plasma interaction.

S Elizer, *"The Interaction of High Power Lasers with Plasmas"*, IOP Series in Plasma Physics (2002)

Part I – Single & Colliding Plasma Basics

Making Stagnation Layers

$$d = \gamma f\left(n-1\right)$$

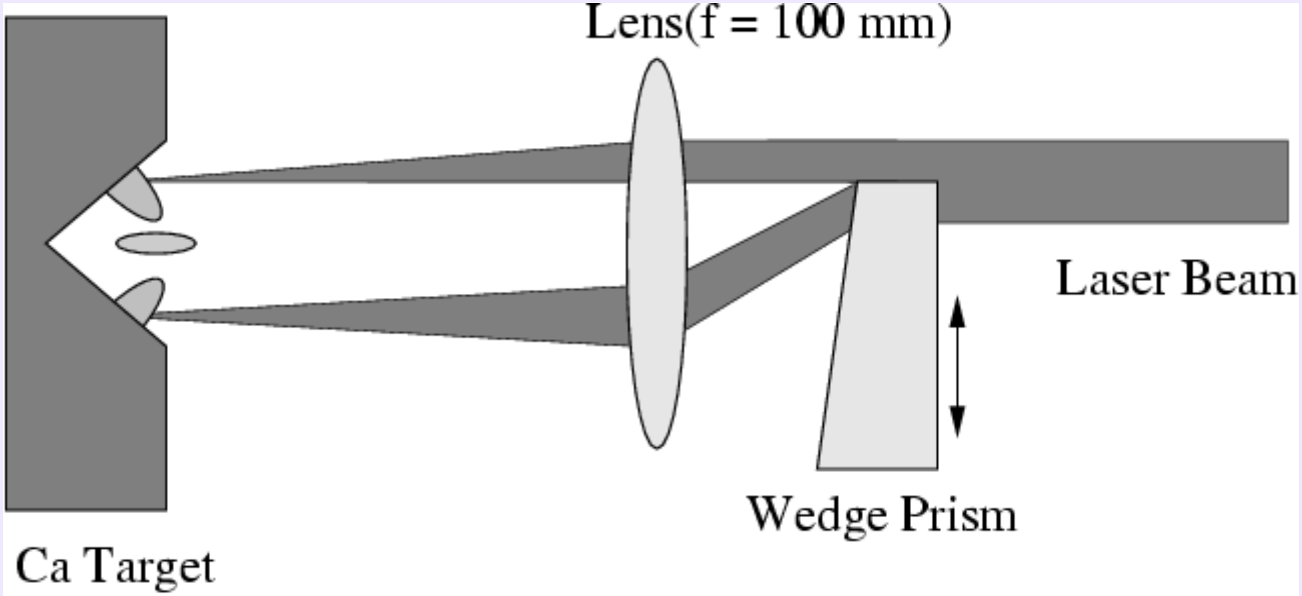

Laser Pulse Energy: 50 - 500 mJ/ beam
Laser Wavelengths: 355nm, 532 nm, 1064 nm
Laser Pulse duration: 170 ps, 6 ns, 15 ns
Focal Spot Size: ~30 - 100 μm
Irradiance: 10^{9} - 10^{11} W.cm^{-2}

Part I – Single & Colliding Plasma Basics

Not a new idea !

Plasma Physics, Vol. 16, pp. 969 to 975. Pergamon Press 1974. Printed in Northern Ireland

INTERACTIONS BETWEEN TWO COLLIDING LASER PRODUCED PLASMAS

P. T. RUMSBY,* J. W. M. PAUL and M. M. MASOUD†
UKAEA Research Group, Culham Laboratory, Abingdon, Berkshire, England

(*Received 29 January* 1974)

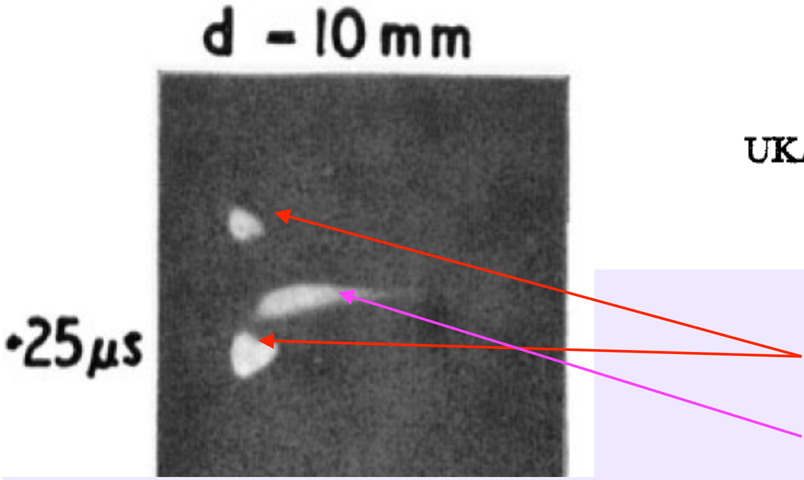

'Seed' Plasmas

'Stagnation Layer'

When plasma plumes collide there are two extreme scenarios:

1. Interpenetration - interactions are mostly via binary collisions
2. Stagnation - plumes decelerated at collision plane, rapid accumulation of material, kinetic energy converted into excitation energy (glow), rapid growth of dense (stagnated) layer,………

Part I – Single & Colliding Plasma Basics

Time Evolution:

Tight point focus on each Ca face:

15 ns/ 120 mJ per 1064 nm beam

ICCD: 5 ns gate
10 ns interval

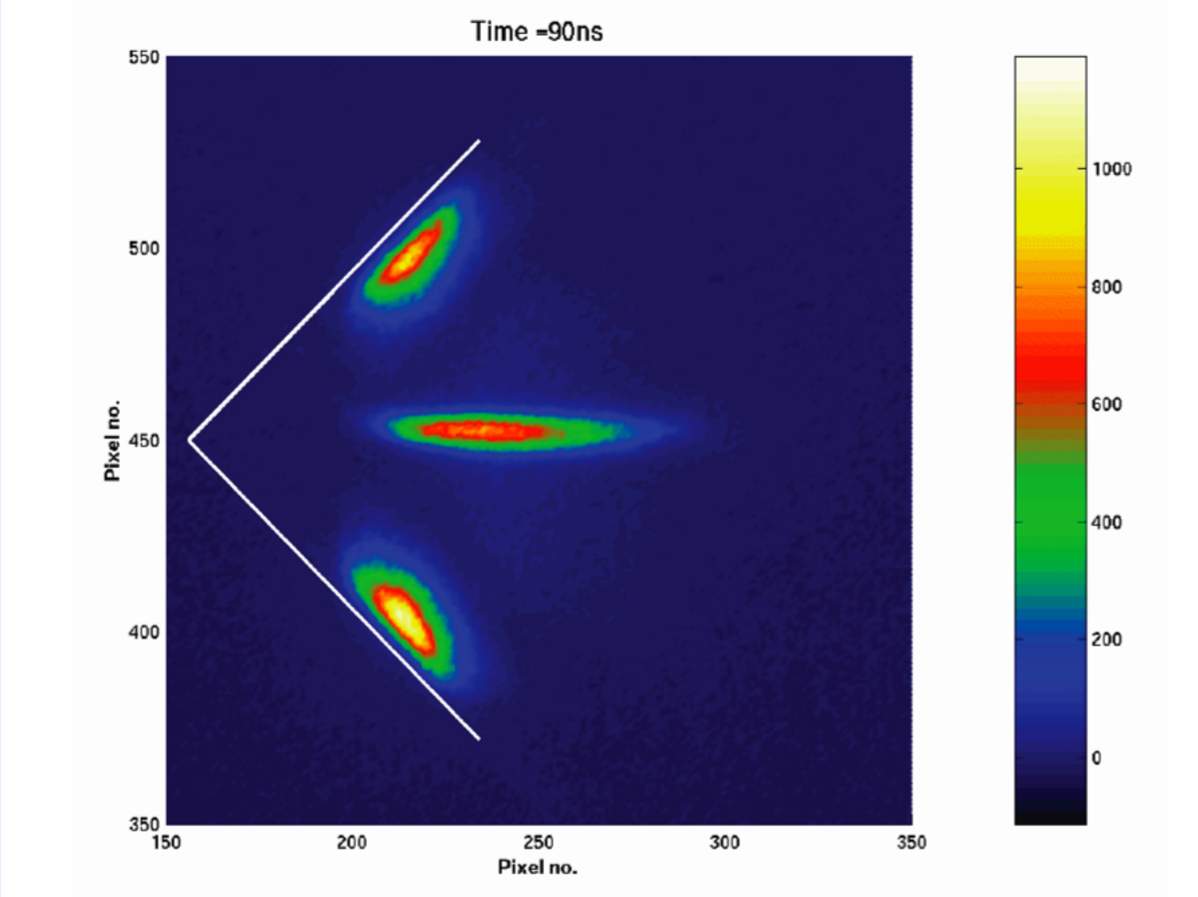

Atomic Ca - Emission Imaging @ 423 nm

H Luna, K D Kavanagh and J T Costello, J. Appl. Phys. **101** Art No 033302 (2007)

Part I – Single & Colliding Plasma Basics

Collisionality Parameter: $\xi = \dfrac{D}{\lambda_{ii}}$

D ← Plasma - Plasma Separation

λ_{ii} ← Ion - Ion Mean Free Path (mfp)

For collisions between opposing plumes (1, 2)

$$\lambda_{ii}(1-2) = \frac{m_i^2 v_{12}^4}{4\pi e^4 Z^4 n_e \ln(\Lambda_{12})}$$

λ_{ii} >> D → Interpenetration
λ_{ii} ~ D → 'Soft' Stagnation
λ_{ii} << D → 'Hard' Stagnation

Slow moving and dense plumes are more likely to stagnate !

P. W. Rambo and J. Denavit, Phys. Plasmas **1** pp 4050 - 4060 (1994)
J Dardis and J T Costello, Spectrochimica Acta Part B **65** pp627-635 (2010)

Part I – Single & Colliding Plasma Basics

Collisionality Parameter: $$\xi = \frac{D}{\lambda_{ii}}$$

D ← Plasma - Plasma Separation

λ_{ii} ← Ion - Ion Mean Free Path (mfp)

For collisions between opposing plumes (1, 2)

$$\lambda_{ii}(1-2) = \frac{m_i^2 v_{12}^4}{4\pi e^4 Z^4 n_e \ln(\Lambda_{12})}$$

Key point: *One can engineer stagnation layer characteristics; 'hardness', density, temperature, shape, etc. by varying geometry (D) and laser-target interaction physics (mfp, λ_{ii}) - application specific…..*

Part I – Single & Colliding Plasma Basics

Collisionality Parameter: $\xi = \dfrac{D}{\lambda_{ii}}$

D ← Plasma - Plasma Separation

λ_{ii} ← Ion - Ion Mean Free Path (mfp)

For collisions between opposing plumes (1, 2)

$$\lambda_{ii}(1-2) = \frac{m_i^2 v_{12}^4}{4\pi e^4 Z^4 n_e \ln(\Lambda_{12})}$$

So perhaps a stagnation layer could be considered to be a 'Plasma Science and Technology Platform' - Laboratory Astrophysics, Hohlraum Physics, plasma XRL Host, PLD are proposed. Others could include pre-heated targets for bright laser plasma light sources (EUVL), LIBS, XFELs…. ?

Part I – Single & Colliding Plasma Basics

S Elizer, *"The Interaction of High Power Lasers with Plasmas"*
Simple scaling law for ion-ion mean free path (H-like plasmas)

$$\lambda_{ii} \sim 5 \times 10^{12}\ T^2\ (eV)/n(cm^{-3})$$

D ~ 1 cm
T ~ 10 eV (max)
n ~ 10^{17} cm^{-3} (typ.)

$$\Rightarrow \lambda_{ii} \sim 5 \times 10^{-3}\ cm$$

$$\zeta_{ii} \sim 200\ (min)$$

State of Simulation in the Literature

Multi-fluid simulation fairly well established - difficult numerical problem especially at plasma vacuum interface - currently developing multifluid code to handle colliding plasmas based on work of:

Rambo and Denavit, J. Comput. Phys. **98** 317 (1992) &
(for experimentalists) Physics of Plasmas **1** 4050 (1994)

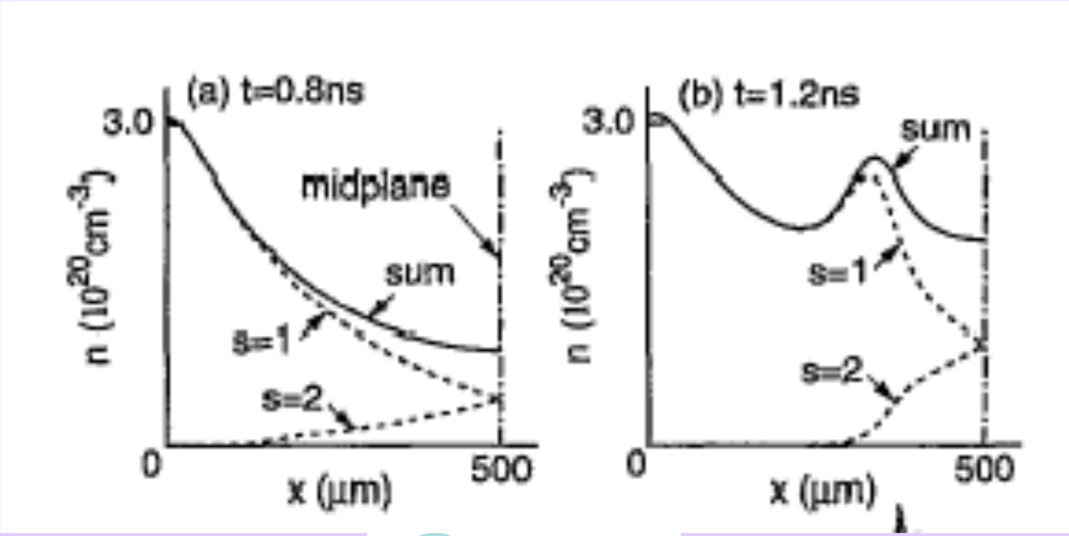

Colliding Al Plasmas
D = 1 mm
$U_{inj} = 3 \times 10^7$ cm/s

Part II – Colliding Plasmas Motivation

Motivations for the study and applications of colliding plasma are many and varied….

Significant body of literature on colliding plasma basics- but mainly on work at high power laser facilities !

1. Fusion (Hohlraums)
2. X-ray Lasers
3. Space Weather Observations
4. Pulsed Laser Deposition
5. Laboratory-Astrophysical Model Experiments

1. T R Dittrich et al., Phys. Plasmas **6** 2164 (1999)
2. R W Clark et al., Phys. Plasmas **4** 3718 (1997)
3. J L Horwitz and T E Moore, IEEE Trans. Plasma. Sci. **28** 1840 (2000)
4. C Sanchez Ake et al., J. Appl. Phys **100** 053305 (2006)
5. C D Gregori et al., Ap. J. **676** 420 (2008)

Part II – Colliding Plasmas Motivation

'Hohlraums – Fusion energy generation'

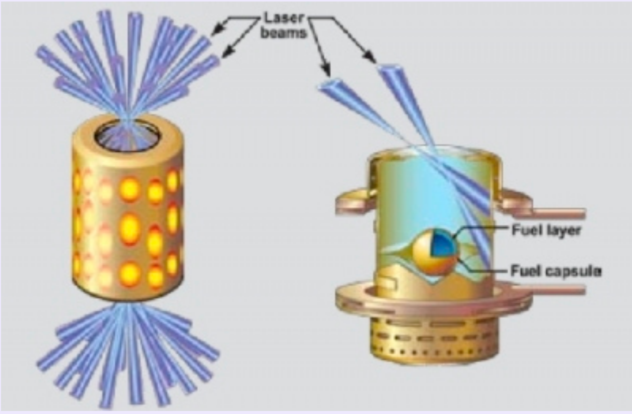

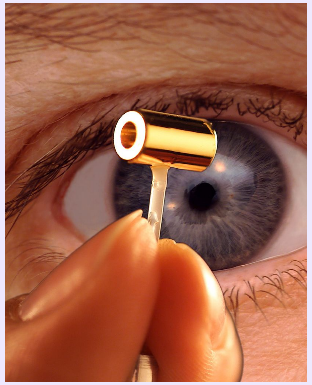

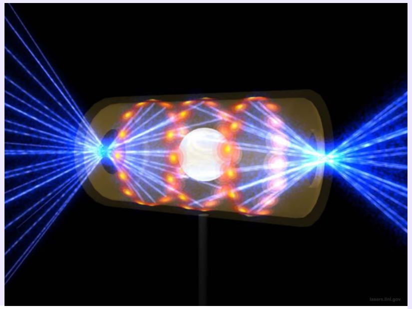

Multiple laser plasmas formed inside a single high-Z cavity e.g., Au) which provide an array of extremely bright X-ray sources. The fuel pellet is compressed by the X-ray radiation pressure. Advantage is more uniform compression with amelioration of instabilities…

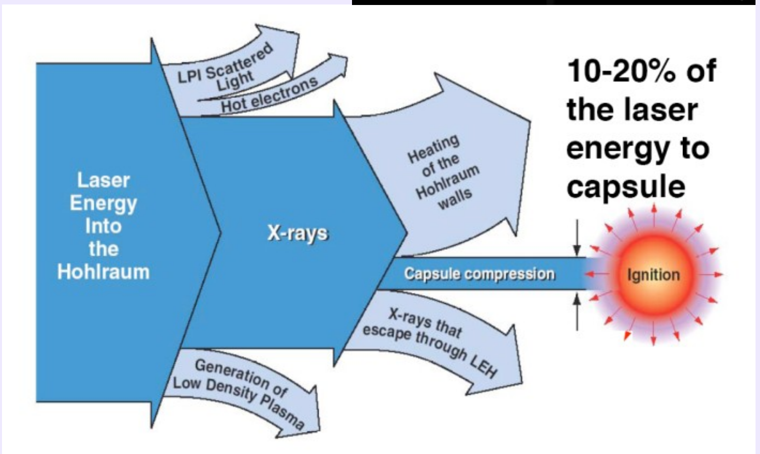

Part II – Colliding Plasmas Motivation

'Hohlraums – Fusion energy generation'

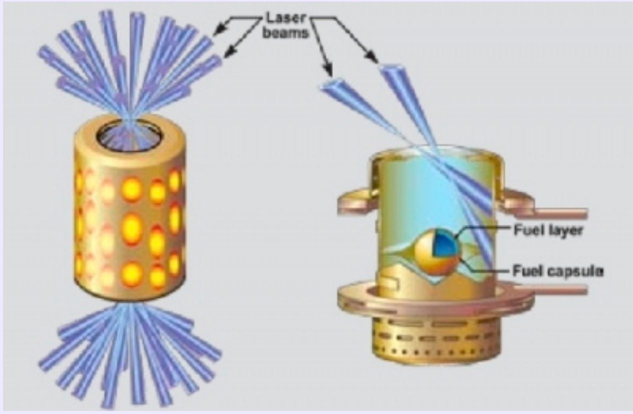

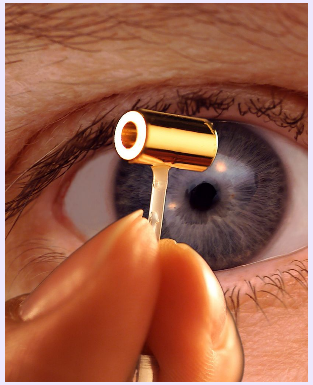

PRL 110, 145005 (2013) PHYSICAL REVIEW LETTERS week ending 5 APRIL 2013

Collisionless Coupling of Ion and Electron Temperatures in Counterstreaming Plasma Flows

J. S. Ross,[1] H.-S. Park,[1] R. Berger,[1] L. Divol,[1] N. L. Kugland,[1] W. Rozmus,[1,2] D. Ryutov,[1] and S. H. Glenzer[1]
[1]*Lawrence Livermore National Laboratory, P. O. Box 808, Livermore, California 94551, USA*
[2]*Department of Physics, University of Alberta Edmonton, Alberta, Canada T6G 2R3*
(Received 22 February 2013; published 2 April 2013)

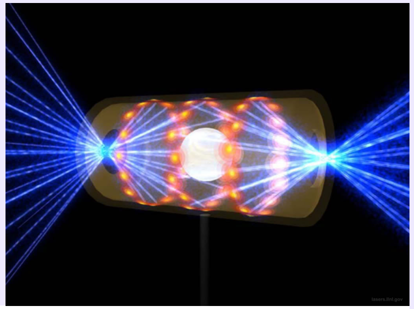

PRL 111, 085003 (2013) PHYSICAL REVIEW LETTERS week ending 23 AUGUST 2013

Experimental Characterization of the Stagnation Layer between Two Obliquely Merging Supersonic Plasma Jets

E. C. Merritt,[1,2] A. L. Moser,[1] S. C. Hsu,[1,*] J. Loverich,[3] and M. Gilmore[2]
[1]*Los Alamos National Laboratory, Los Alamos, New Mexico 87545, USA*
[2]*University of New Mexico, Albuquerque, New Mexico 87131, USA*
[3]*Tech-X Corporation, Boulder, Colorado 80303, USA*
(Received 22 March 2013; published 22 August 2013)

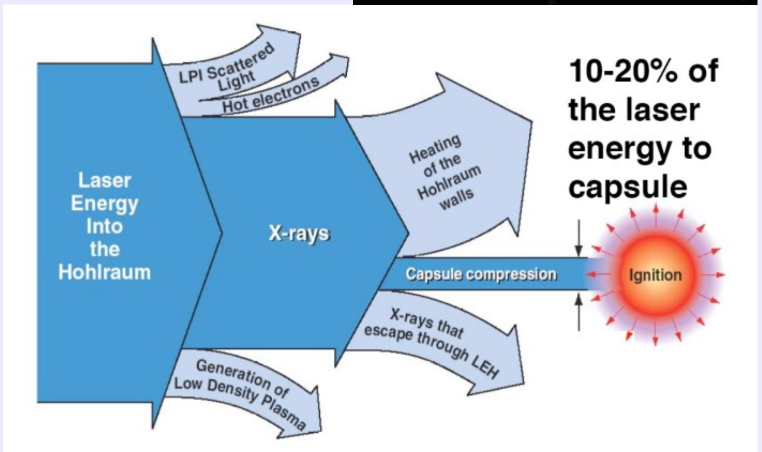

Part II – Colliding Plasmas Motivation

'Colliding Stars'

NGC2346 -
Planetary Nebula
Distance - 2,000 light years
Extent ~ 0.4 light years

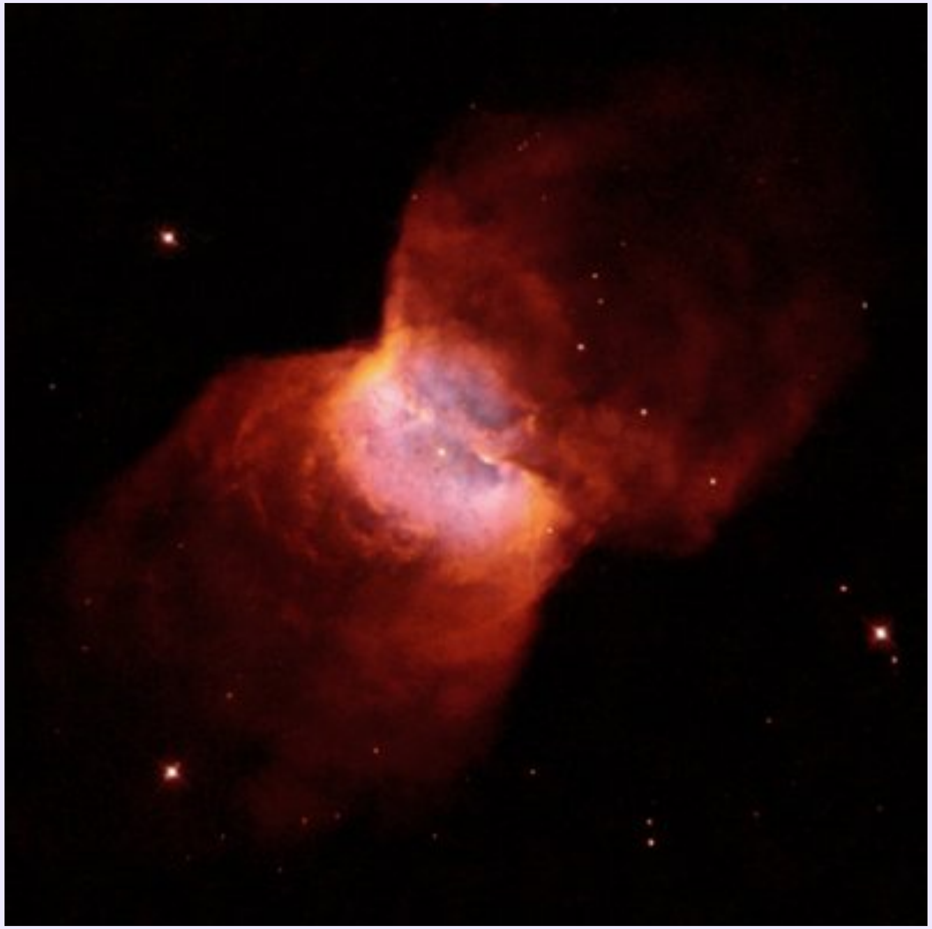

Result of the collision of two stars – believed that one became a red giant and swallowed its partner in the binary system.

Credit: Hubble Wide Field & Planetary Camera - Massimo Stiavelli (NASA)

Part III – SL Diagnostics

Stagnation layer growth (evolution)

Time resolved (ICCD) imaging

1. Time-space resolved spectroscopy

Plasma Parameterisation

1. Time-space resolved spectroscopy - n_e & T_e
2. Time resolved interferometry - n_e
3. Time resolved shadowgraphy – shock detection
4. Faraday cup - angle resolved ion current – $i(\theta)$

D Doria, K D Kavanagh, J T Costello and H Luna, Meas. Sci. Technol. **17** 670 (2006)

P Hough, T J Kelly, C Fallon, C McLoughlin, P Hayden, E T Kennedy, J-P Mosnier, S S Harilal and J T Costello, Meas. Sci. Technol. **23** 125204 (2012)

P Yeates, C Fallon, E T Kennedy and J T Costello, Physics of Plasmas **20**, 093106 (2013)

Part III – SL Diagnostics

Stagnation layer evolution/parameterisation

1. Fast Photography - all phases (0 – 1000 ns)
2. Interferometry - usable early phase (0 – 100 ns)
3. Spectroscopy - usable mid phase (50 - 500 ns)
4. Faraday cup - ions and electrons
5. Others: Shadowgraphy, Moire deflectometry, etc.

D Doria, K D Kavanagh, J T Costello and H Luna, Meas. Sci. Technol. **17** 670 (2006)

P Hough, T J Kelly, C Fallon, C McLoughlin, P Hayden, E T Kennedy, J-P Mosnier, S S Harilal and J T Costello, Meas. Sci. Technol. **23** 125204 (2012)

P Yeates, C Fallon, E T Kennedy and J T Costello, Physics of Plasmas **20**, 093106 (2013)

Part III – SL Diagnostics

Experimental Geometry for ICCD Photography:

Time and angle resolved.

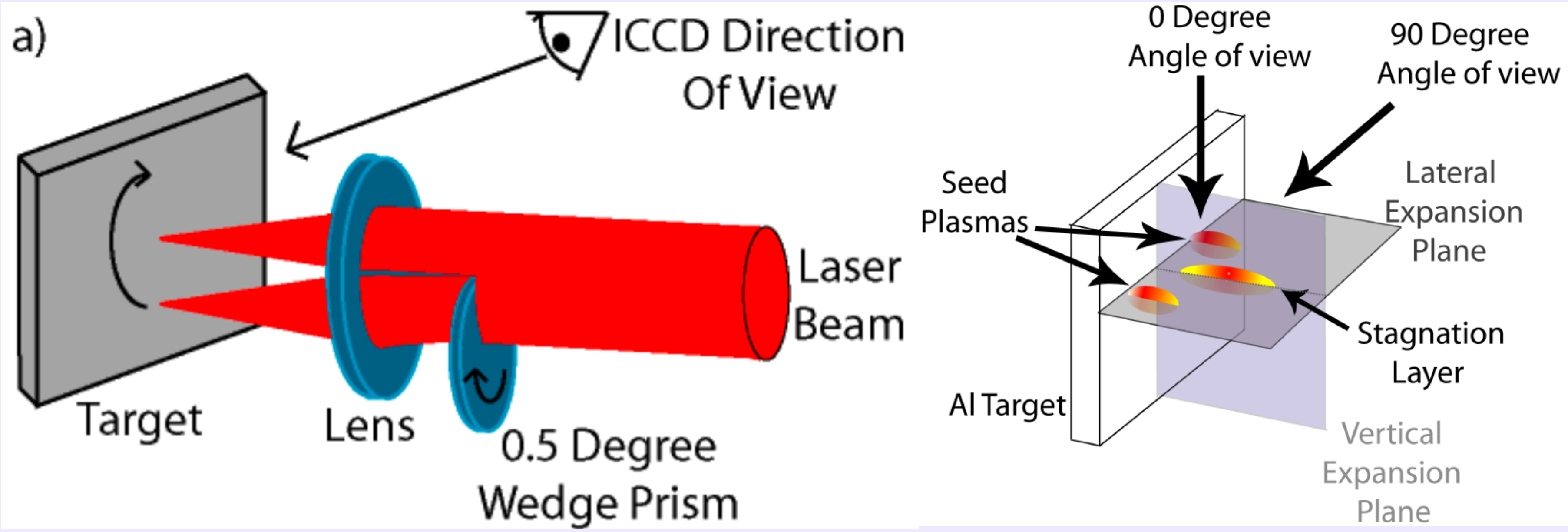

P Hough, C McLoughlin, S S Harilal, J-P Mosnier and J T Costello, J. Appl. Phys **107** 024904 (2010)

Part III – SL Diagnostics

ICCD Photography: Time and angle resolved.

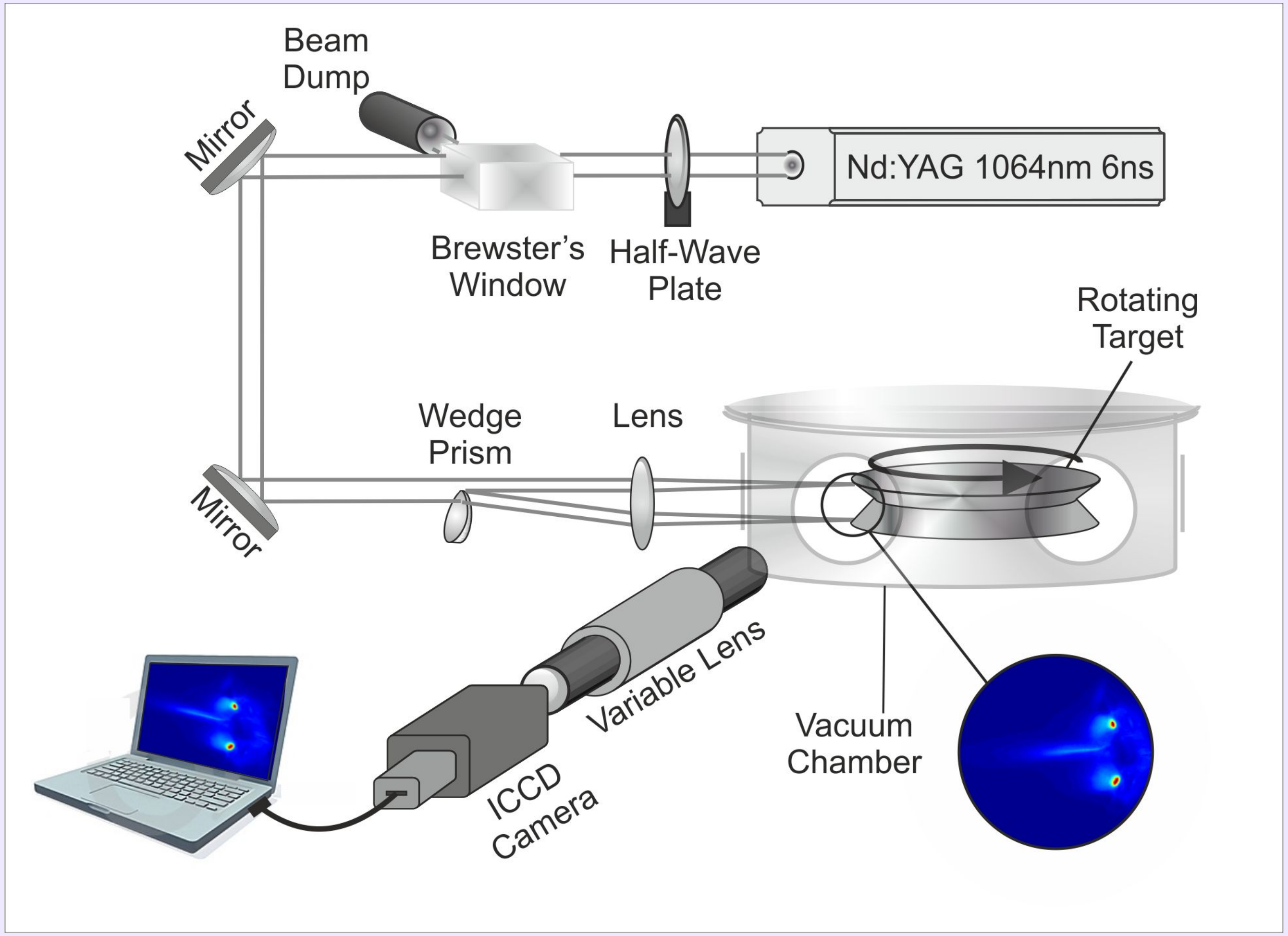

C Fallon, P Hayden, N Walsh, E T Kennedy and J T Costello,
Journal of Physics: Conference Series **548** 012036 (2014)

Part III – SL Diagnostics

ICCD Spectroscopy: Time and space resolved.

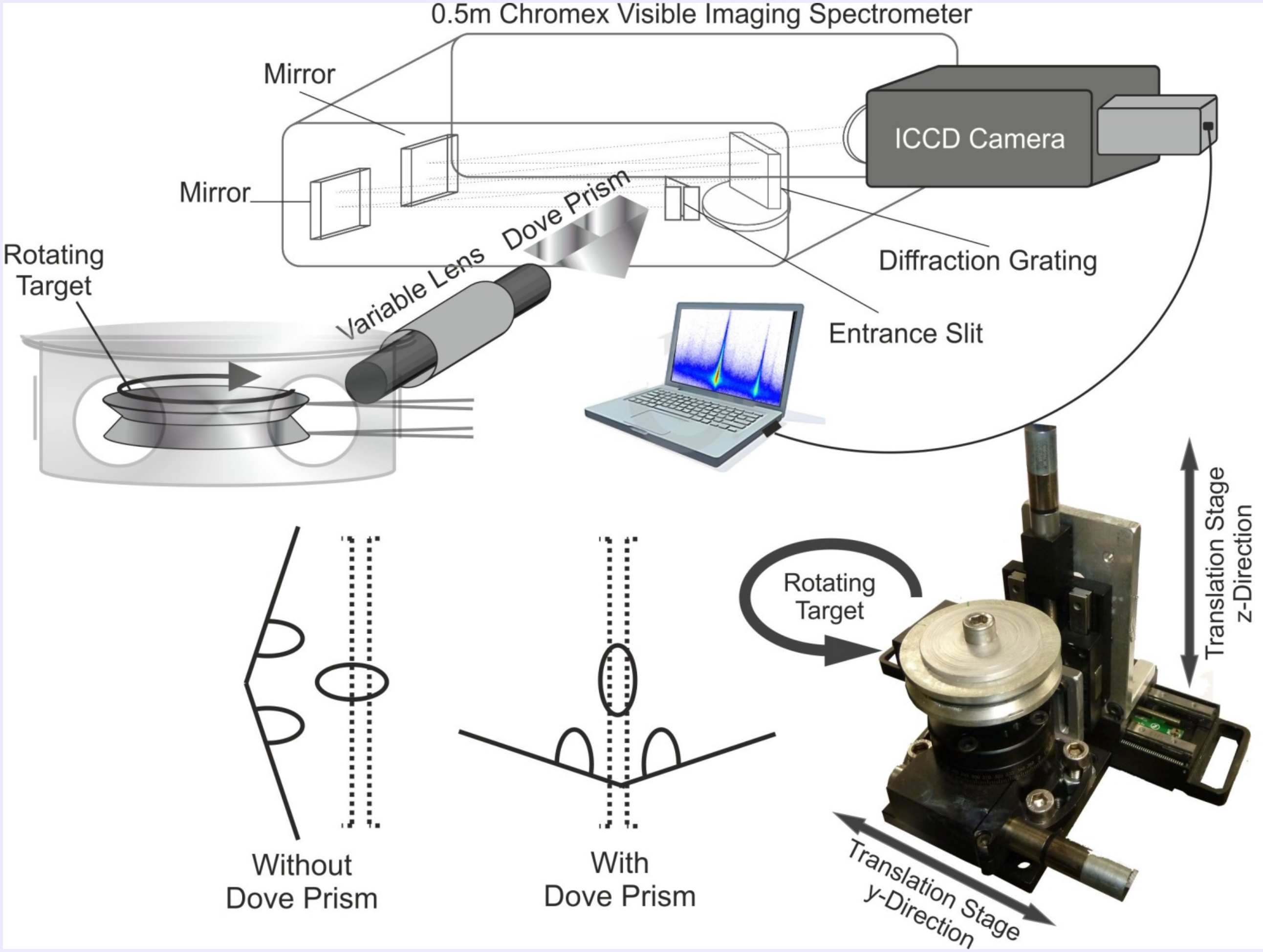

C Fallon, P Hayden, N Walsh, E T Kennedy and J T Costello,
Physics of Plasmas (Submitted, Jan 2015)

Part III – SL Diagnostics

First Bespoke Colliding Plasma Laboratory - (Padraig Hough)
Imaging, Spectroscopy, Interferometry, RETOF,….

Part III – SL Diagnostics

Spectroscopy and Imaging of Ca^+ at 393 nm, $4s_{1/2} - 4p_{1/2,3/2}$

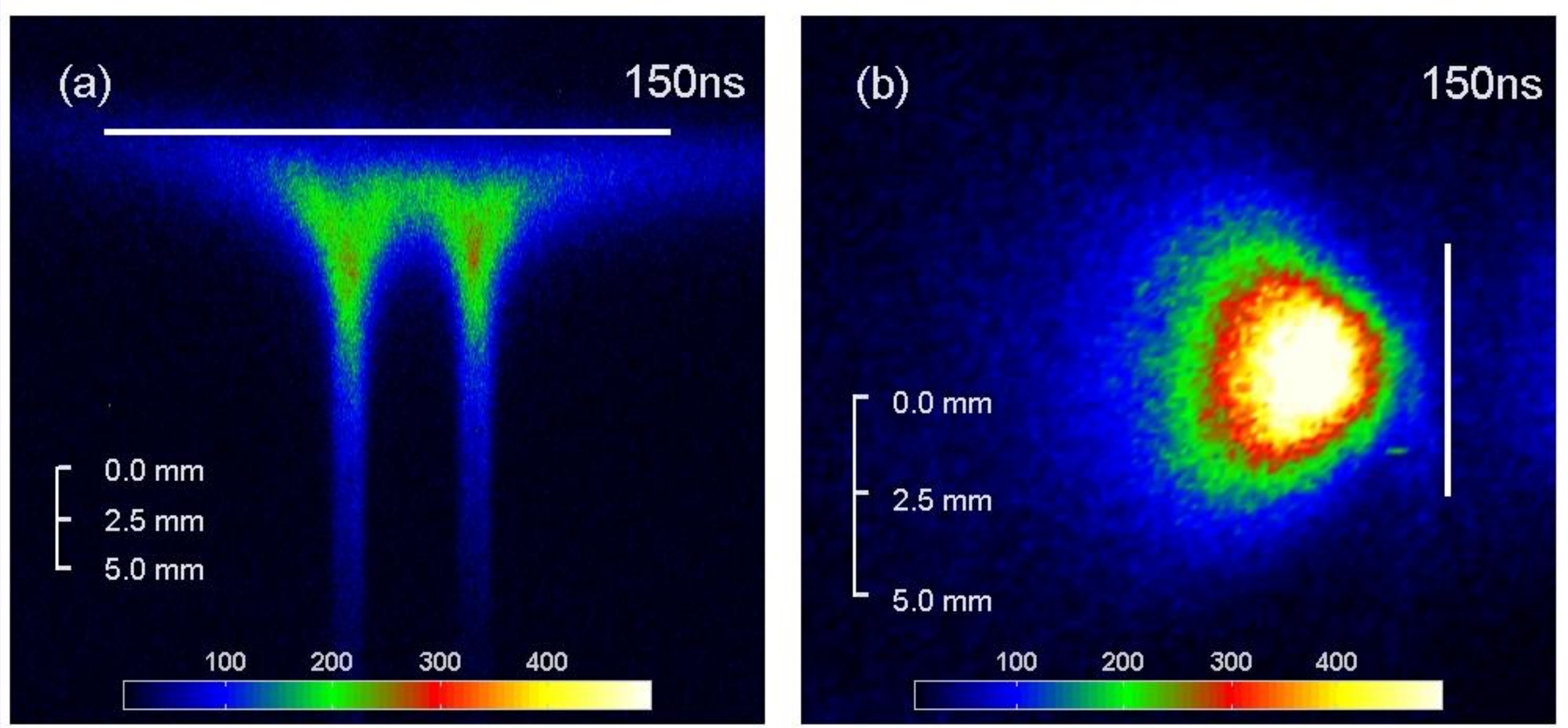

Plasma streaming up along the slit - can use to extract plasma parameters and for ion/electronic state selected species tracking

Imaging with a narrow bandpass filter yields charge state (often electronic state) selected spatial distribution

Part III – SL Diagnostics

Broadband image at 200ns   Colliding aluminium plasmas

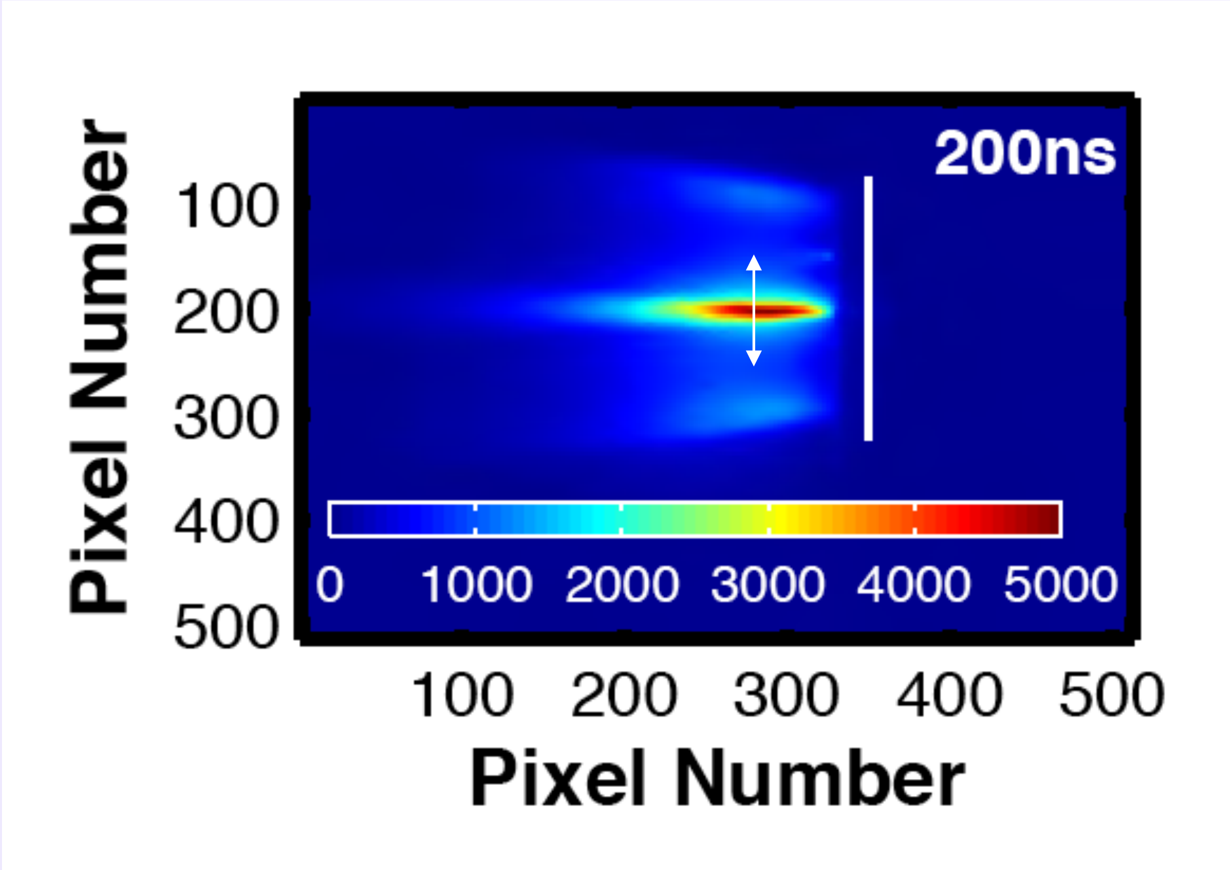

~100 mJ/170 ps/'Seed' Beam (SBS compressed EKSPLA)

Part III – SL Diagnostics

Stagnation Layer Evolution

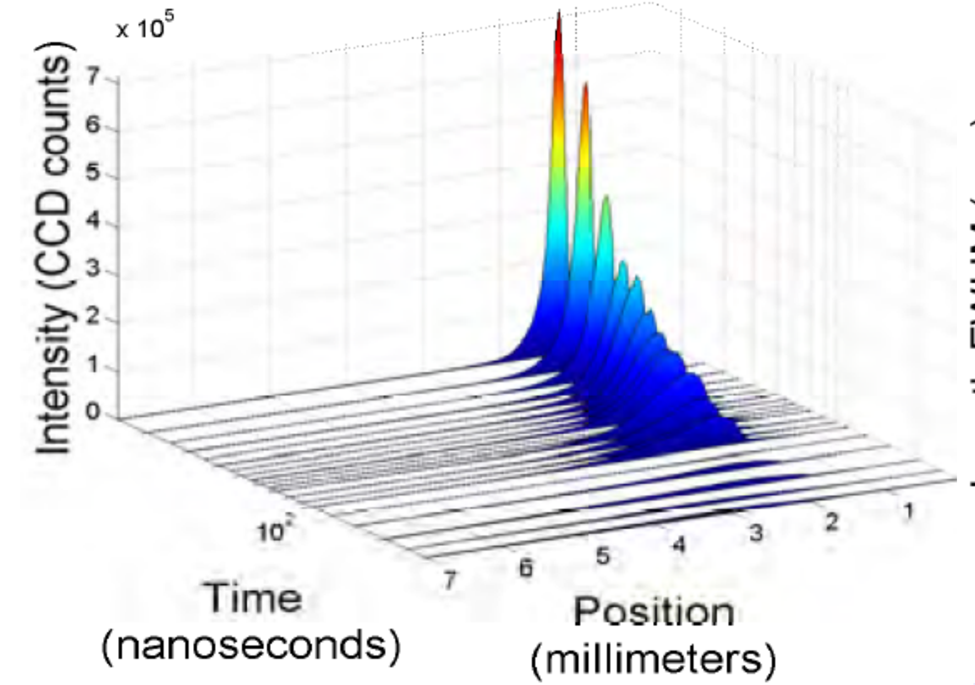

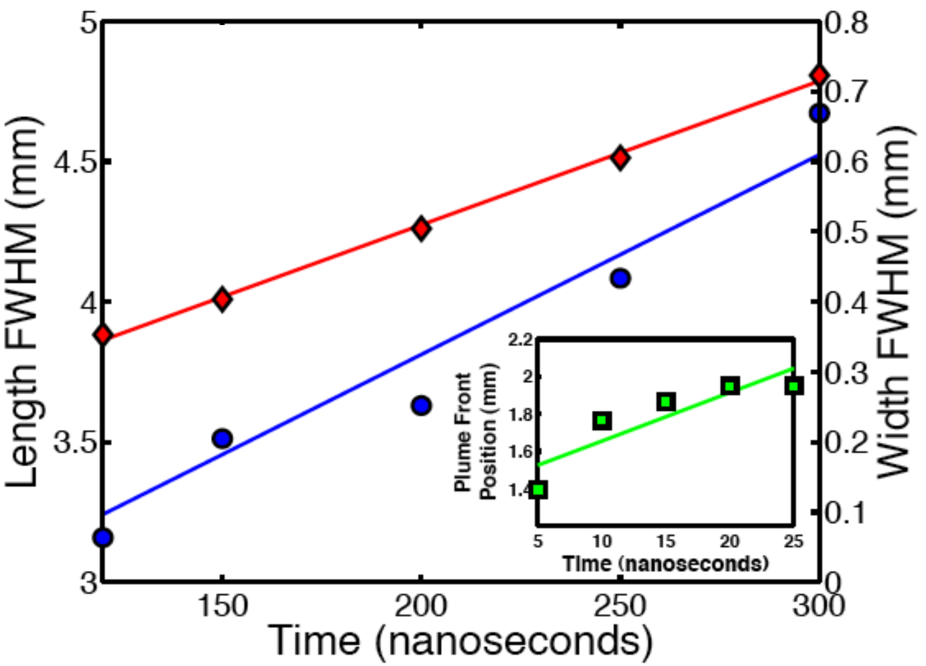

Colliding aluminium plasmas ~100 mJ/170 ps/'seed' beam

Part III – SL Diagnostics

Colliding Aluminium Plasmas - Individual Fluid Asymmetry - cf: Al^+

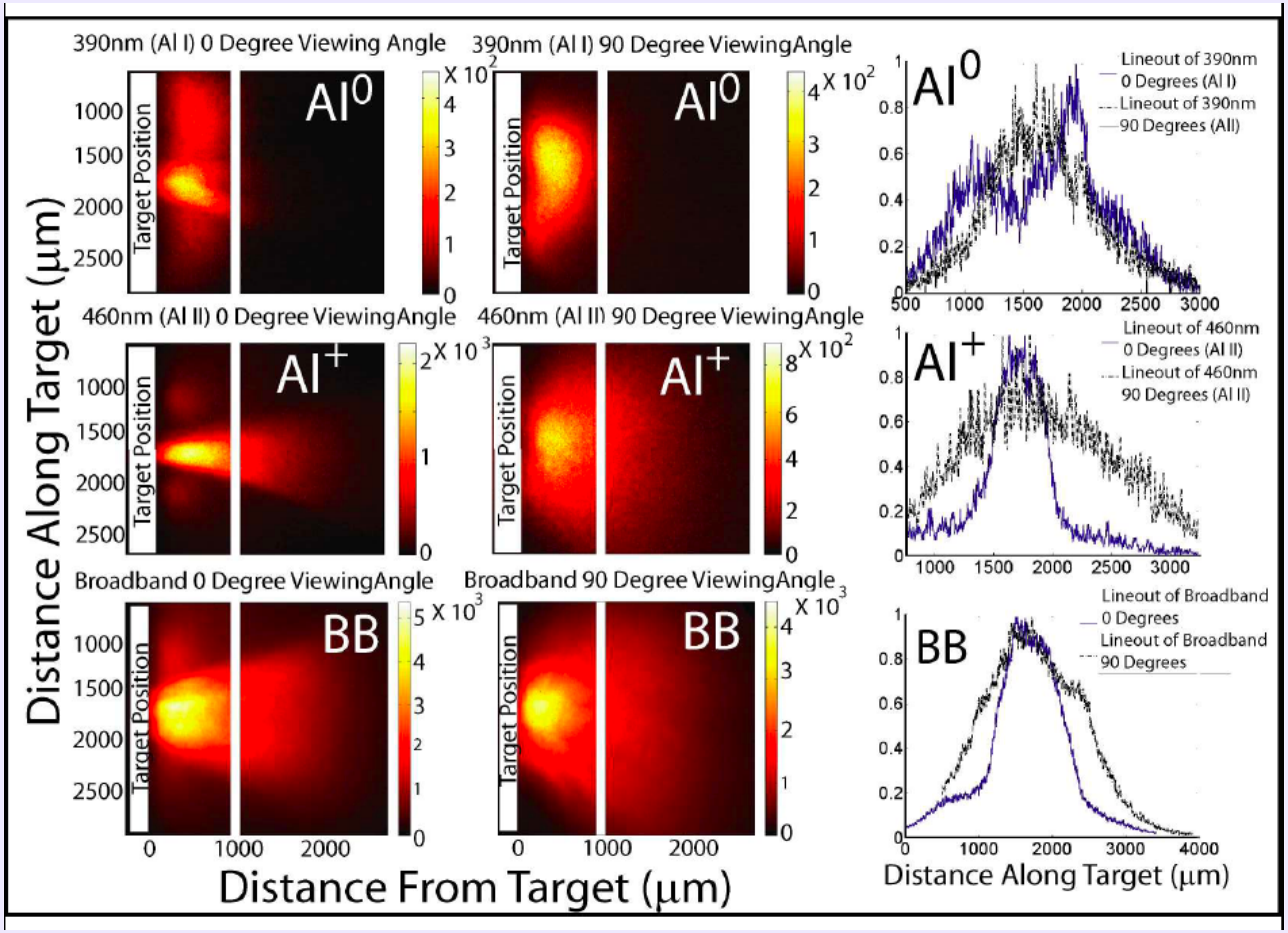

Angle Resolved Imaging:

Al, Al^+ & Broadband

~300 mJ/ 6 ns/ 1064 nm 'seed' beam

P Hough, C McLoughlin, S S Harilal, J-P Mosnier and J T Costello, J. Appl. Phys. **107** 024904 (2010)

Part III – SL Diagnostics

Imaging - effect of seed collision angle

$$\xi = \frac{D}{\lambda_{ii}}$$

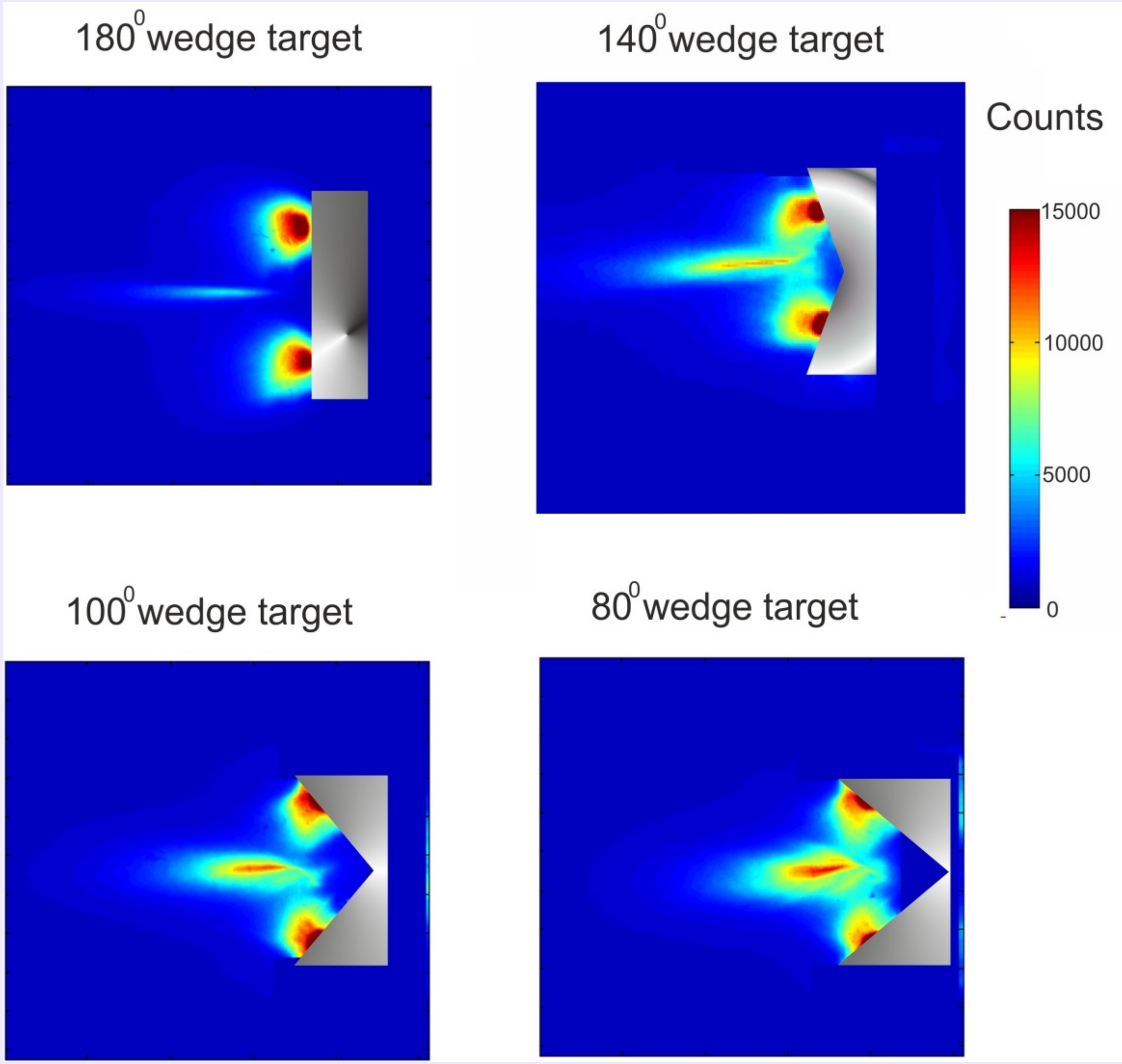

$$\lambda_{ii}(1-2) = \frac{m_i^2 v_{12}^4}{4\pi e^4 Z^4 n_e \ln(\Lambda_{12})}$$

C Fallon, P Hayden, N Walsh, E T Kennedy and J T Costello, J. Phys: Conference Series **548** 012036 (2014)

Time, Space and Angle-Resolved UV-Vis Spectroscopy

Stigmatic Spectrometer + ICCD

Part III – SL Diagnostics

*Stagnation layer **parallel** to spectrometer slit (Al)*

Spectograph

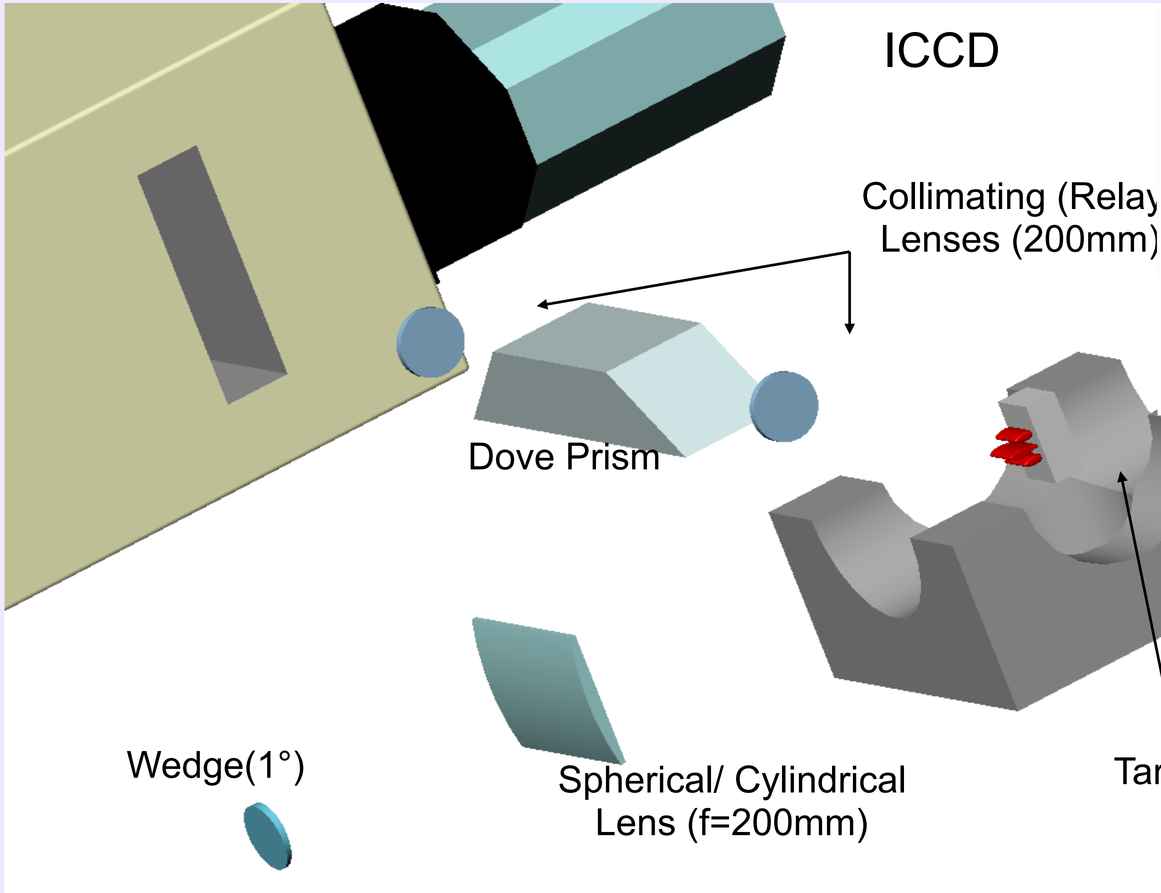

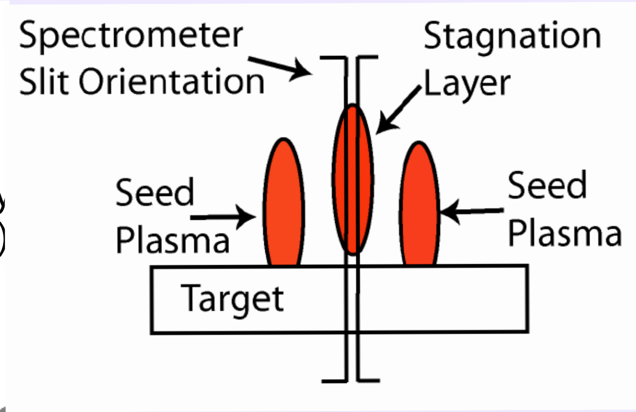

Chamber

Min. gate width = 1.5 ns
Spatial Res. = 70 μm
Spectral Res. <0.2nm

D Doria, K D Kavanagh, J T Costello and H Luna, Meas Sci Technol **17** 670 (2006)

Part III – SL Diagnostics

Al target - ~300 mJ/ 6 ns/ 'seed' beam

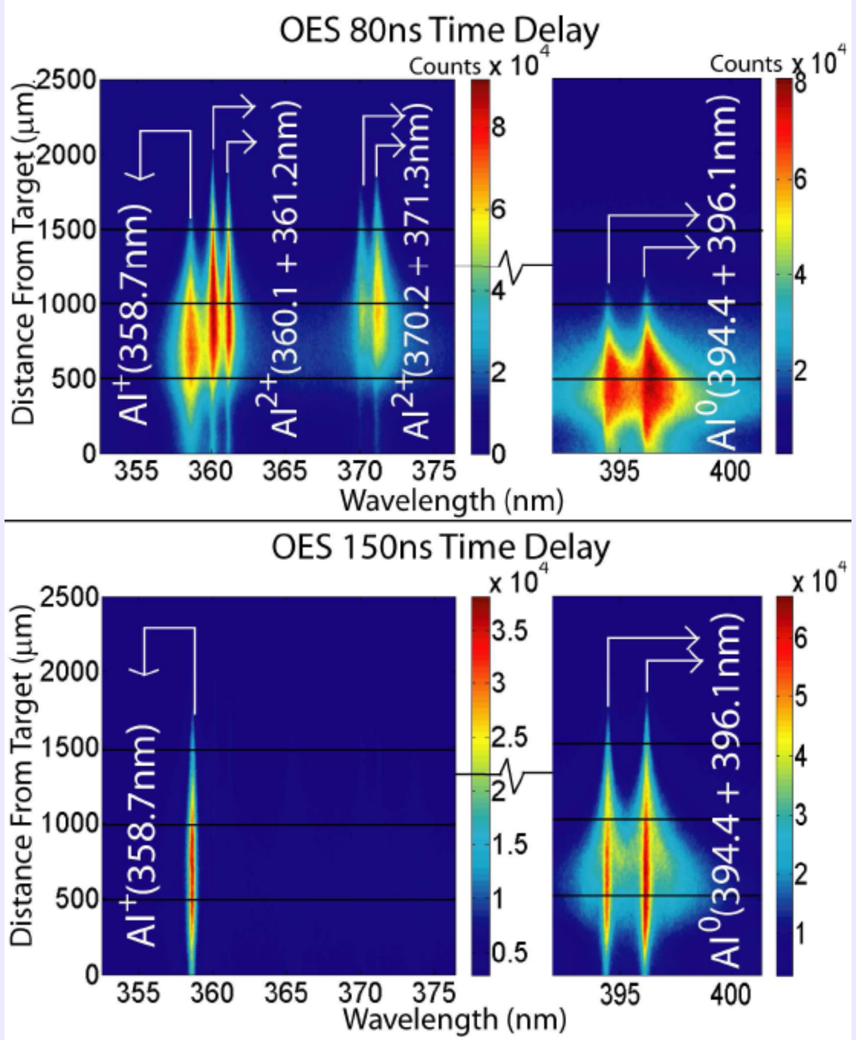

'Growth rate' - 10 μm/ns

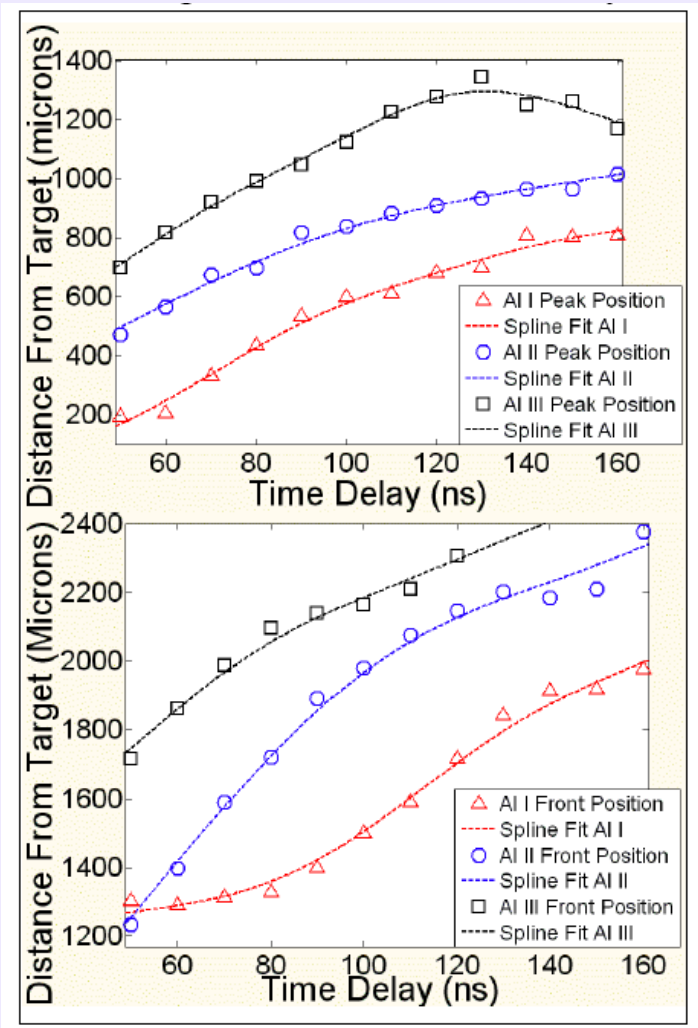

Part III – SL Diagnostics

Extracting Densities and Temperatures

Get densities from Stark broadened lines
– assume electron collisions dominant -

$$\Delta\lambda_{\text{width}} = 2W(Ne/10^{16}) + 3.5A(Ne/10^{16})^{1/4} \times (1 - 1.2N_D^{-1/3})W(Ne/10^{16}),$$

Then temperatures from line intensity ratio for
successive ions stages - assumes LTE

$$\frac{I'}{I} = \frac{f'g'\lambda^3}{fg\lambda'^3}(4\pi^{3/2}a_0^3 Ne)^{-1}\left(\frac{kT}{E_H}\right)^{3/2}\exp\left(\frac{E - E' - E_\infty}{kT}\right)$$

Part III – SL Diagnostics

Stagnation Layer (Al): Electron density (Stark Analysis)

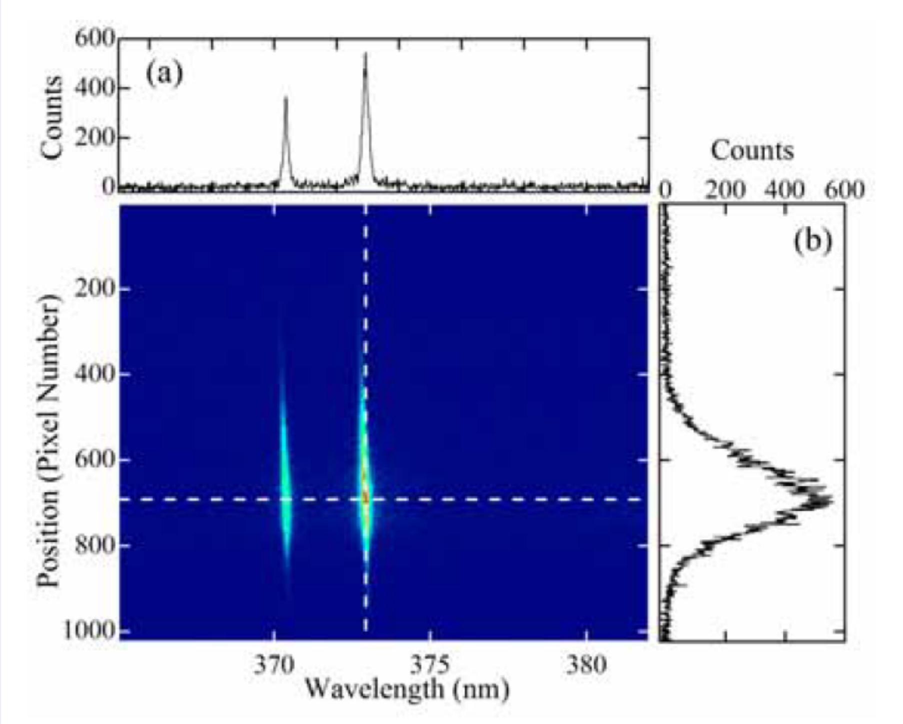

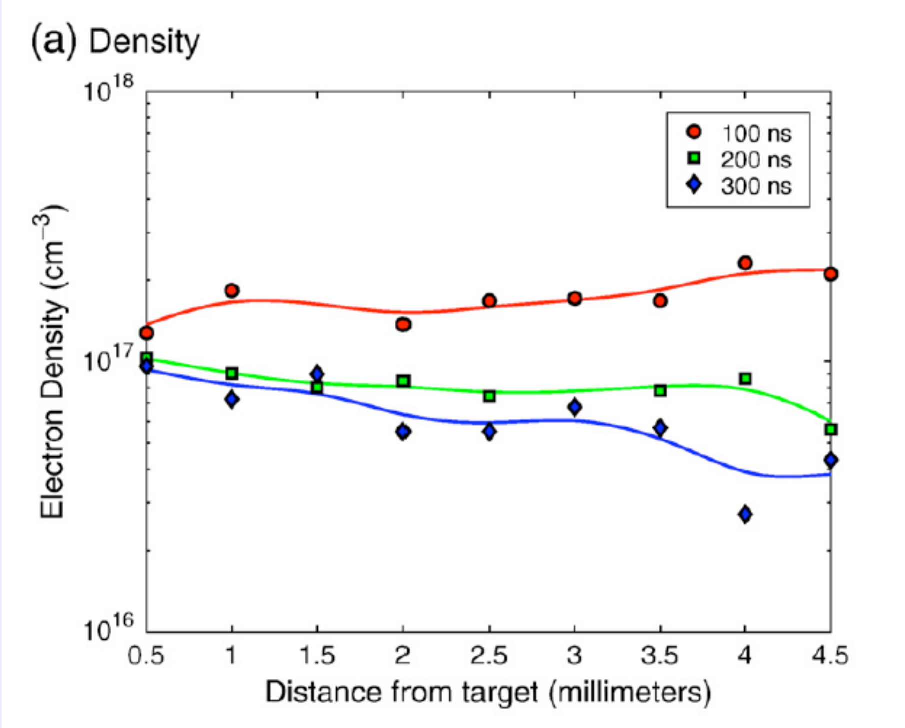

~100 mJ/170 ps/1064 nm 'seed' beam

J Dardis and J T Costello, Spectrochimica Acta Part B **65** pp627-635 (2010)

Part III – SL Diagnostics

Stagnation Layer (Ca): *Electron density (Stark Analysis)*

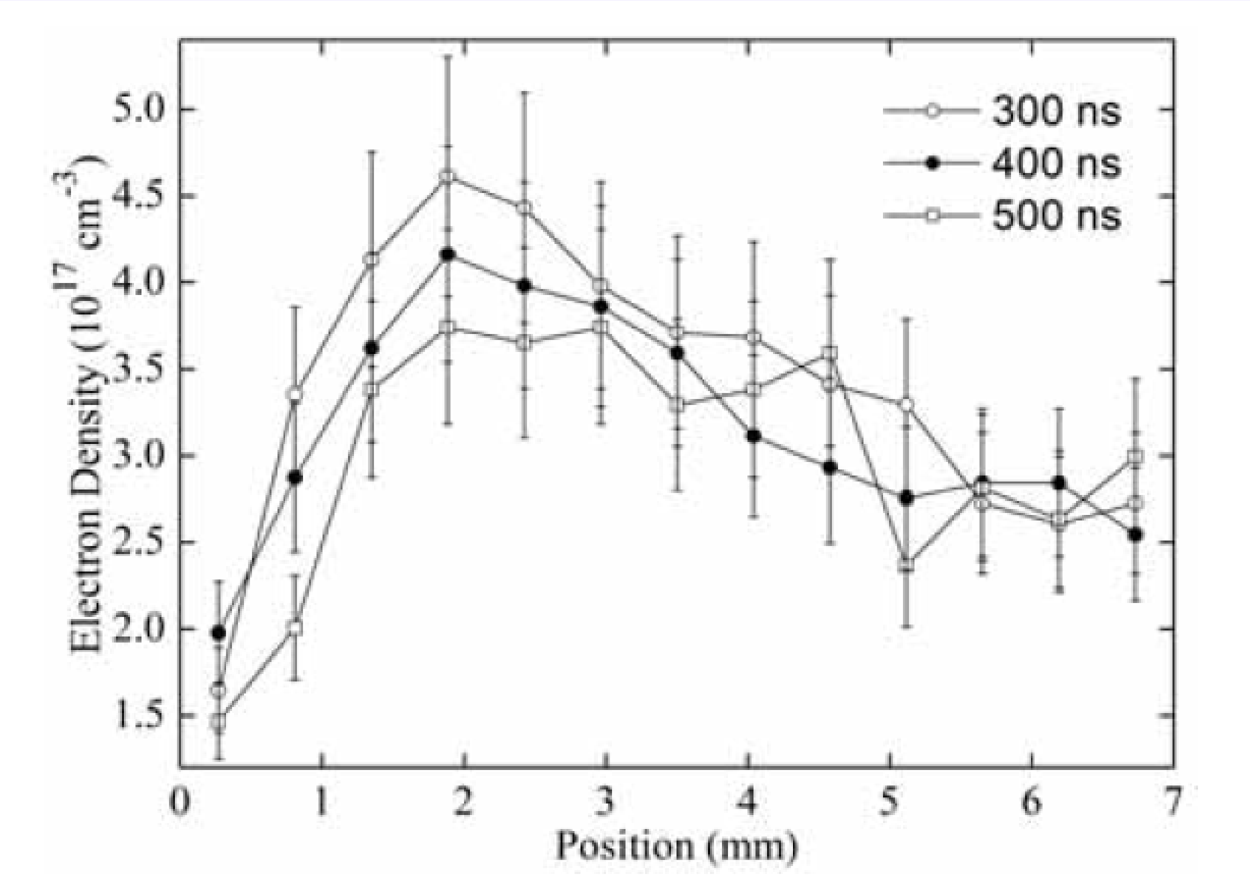

~70 mJ/**355 nm**/
6 ns/ 'seed' beams

$$n_e \approx 3x10^{17}\,cm^{-3}$$

Part III – SL Diagnostics

Stagnation Layer (Ca): *Electron Temp. – Line ratios*

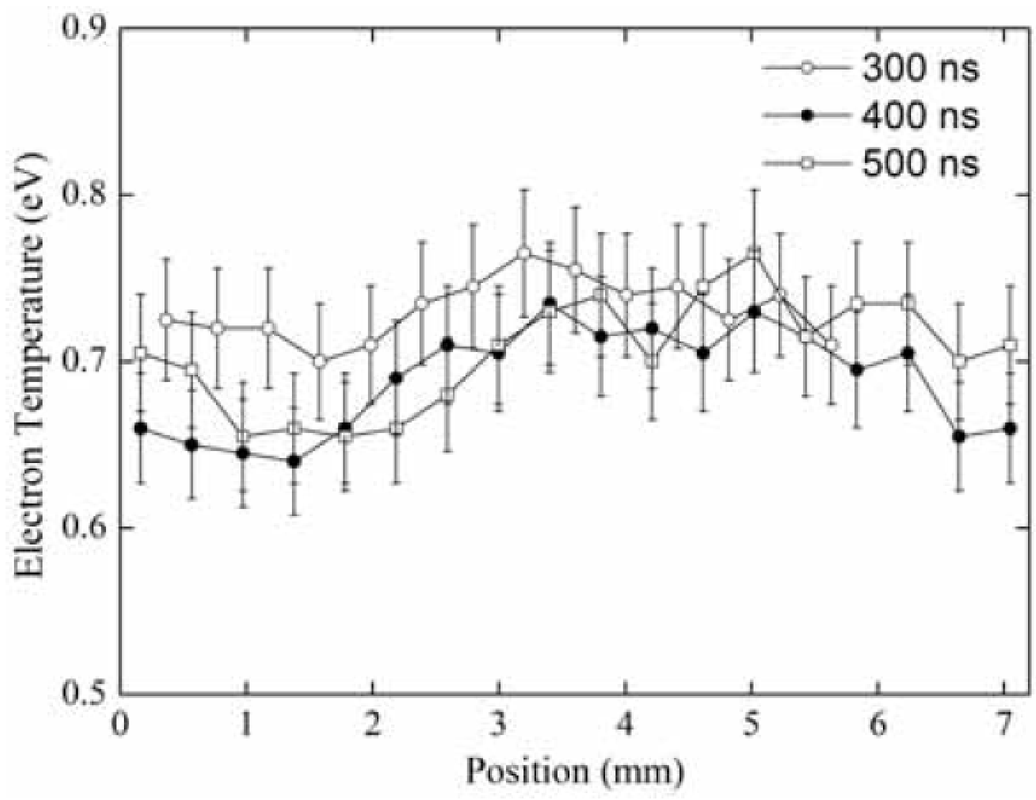

~70 mJ/**355 nm**/
6 ns/ 'seed' beam

$$T_e \approx 0.7eV$$

Ratio of 393 nm (Ca+) to 423 nm (Ca) lines

$$\frac{I'}{I} = \frac{f'g'\lambda^3}{fg\lambda'^3}(4\pi^{3/2}a_0^3 Ne)^{-1}\left(\frac{kT}{E_H}\right)^{3/2}\exp\left(\frac{E - E' - E_\infty}{kT}\right)$$

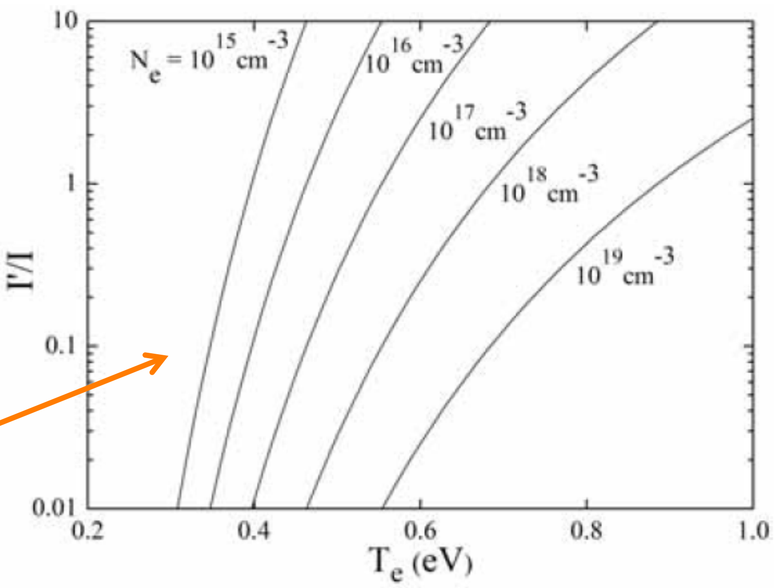

Imaging - effect of seed collision angle

$$\xi = \frac{D}{\lambda_{ii}}$$

$$\lambda_{ii}(1-2) = \frac{m_i^2 v_{12}^4}{4\pi e^4 Z^4 n_e \ln(\Lambda_{12})}$$

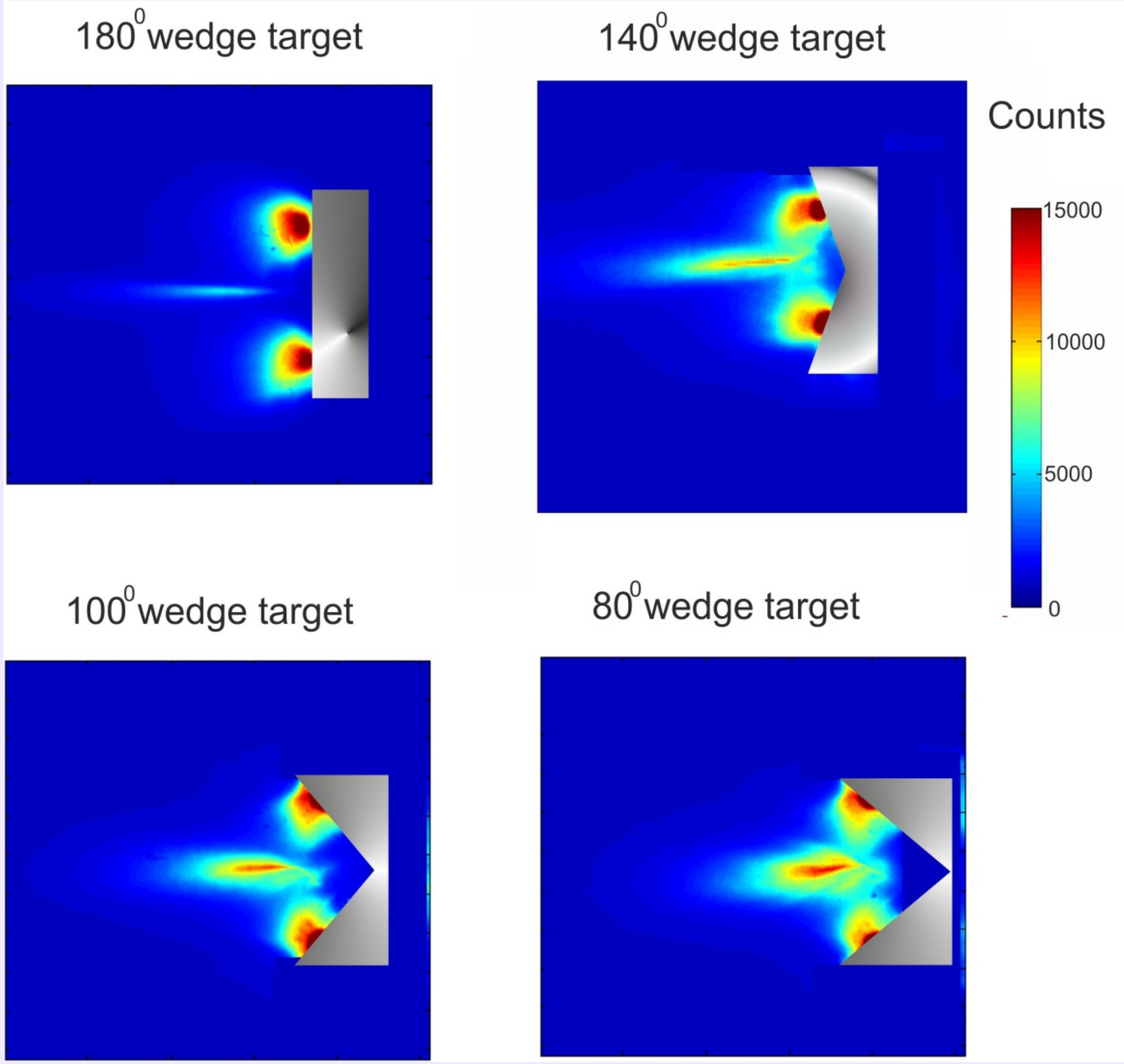

Part III – SL Diagnostics

Copper stagnation layers – Electron densities (Stark widths)

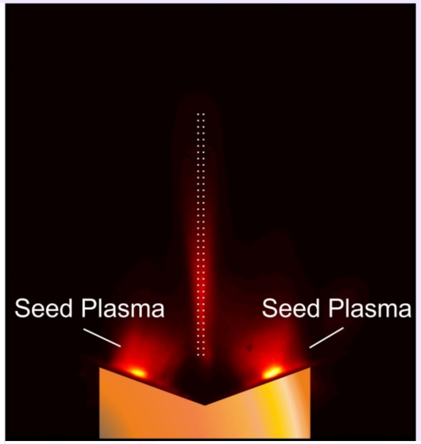

Wedge Angle: 140^{O}

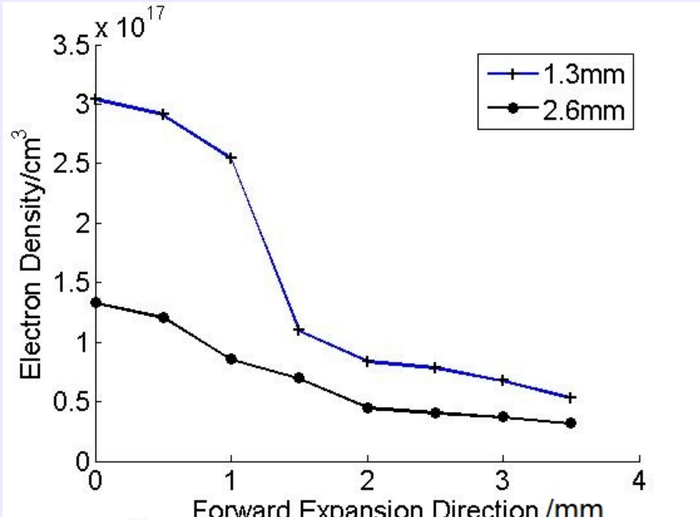

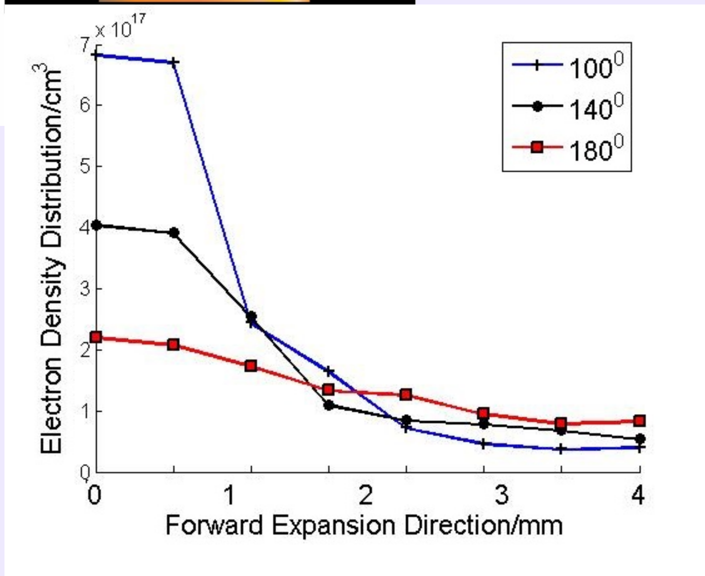

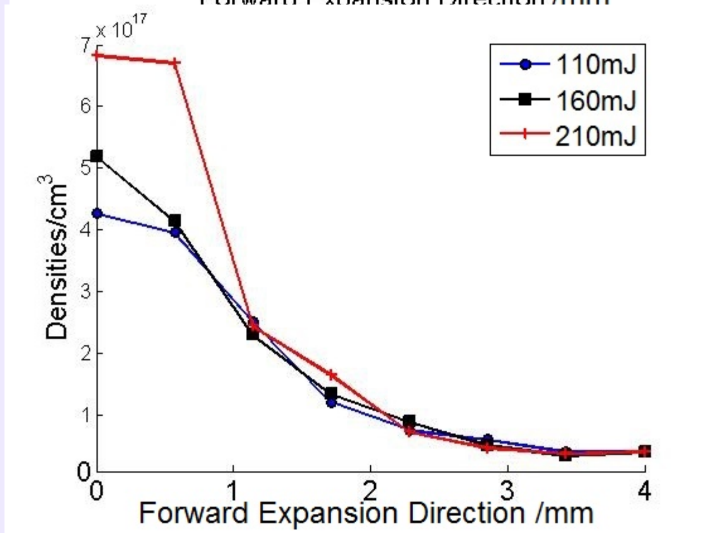

Part III – SL Diagnostics

Copper stagnation layers – Temperatures (Boltzmann Plot)

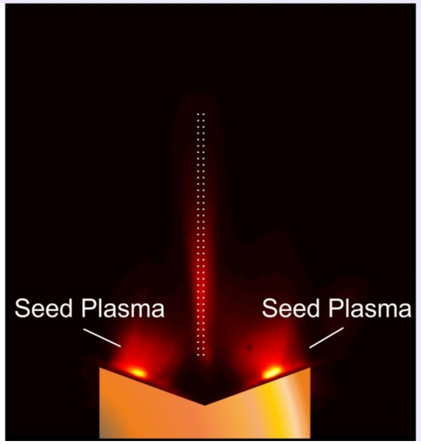

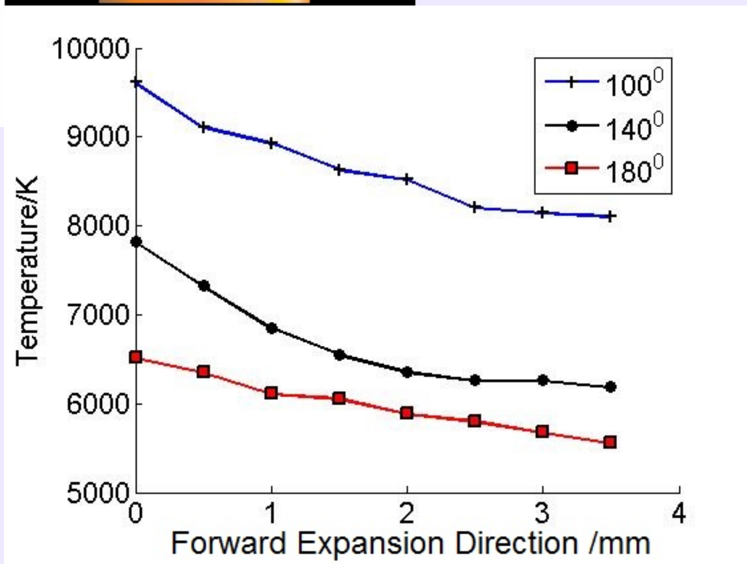

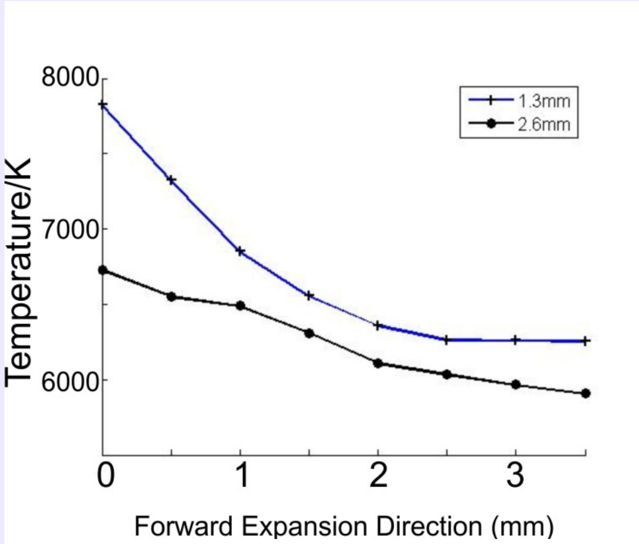

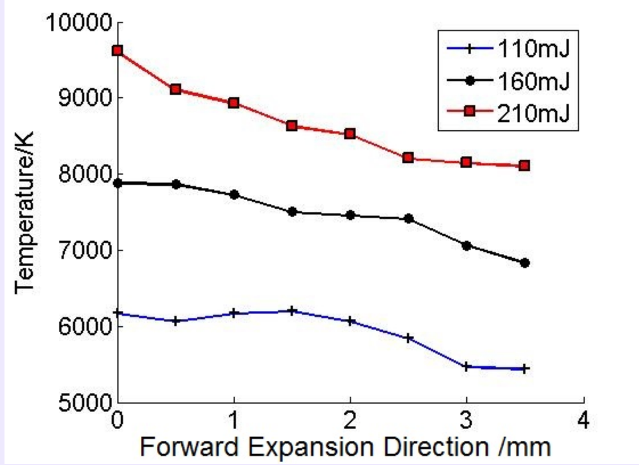

Part III – SL Diagnostics

Stagnation Layer (Al): *Electron density & temperature*

Spectroscopy - only works well for Δt > 100 ns

Spectra dominated by continuum emission - *solution* - *time resolved interferometry*

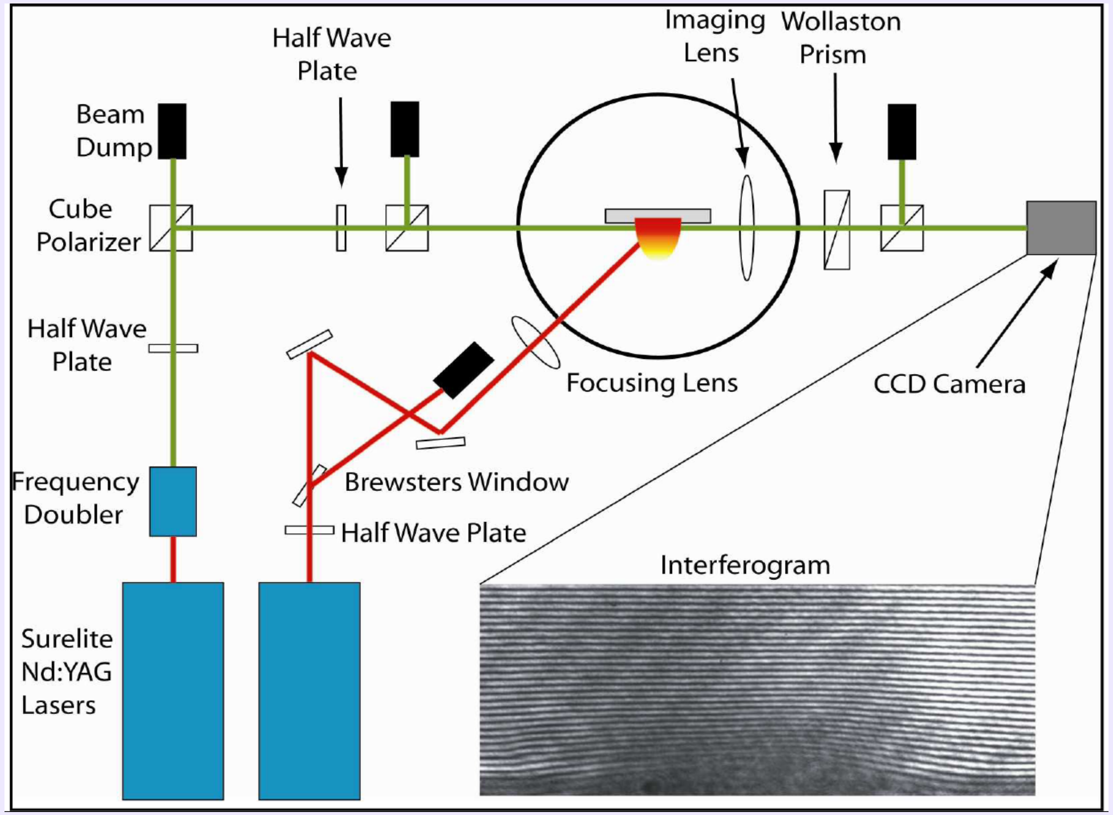

Experimental Setup-

Nomarski Interferometer

P Hough, C McLoughlin, T J Kelly, S S Harilal, J-P Mosnier and J T Costello, Appl. Surf. Sci. **255** 5167 (2009)

Part III – SL Diagnostics

Electron Stagnation at the Collision Plane

P Hough, C McLoughin, T J Kelly, S S Harilal, J P Mosnier and J T Costello, J. Phys. D: Appl. Phys. **42** 055211 (2009)

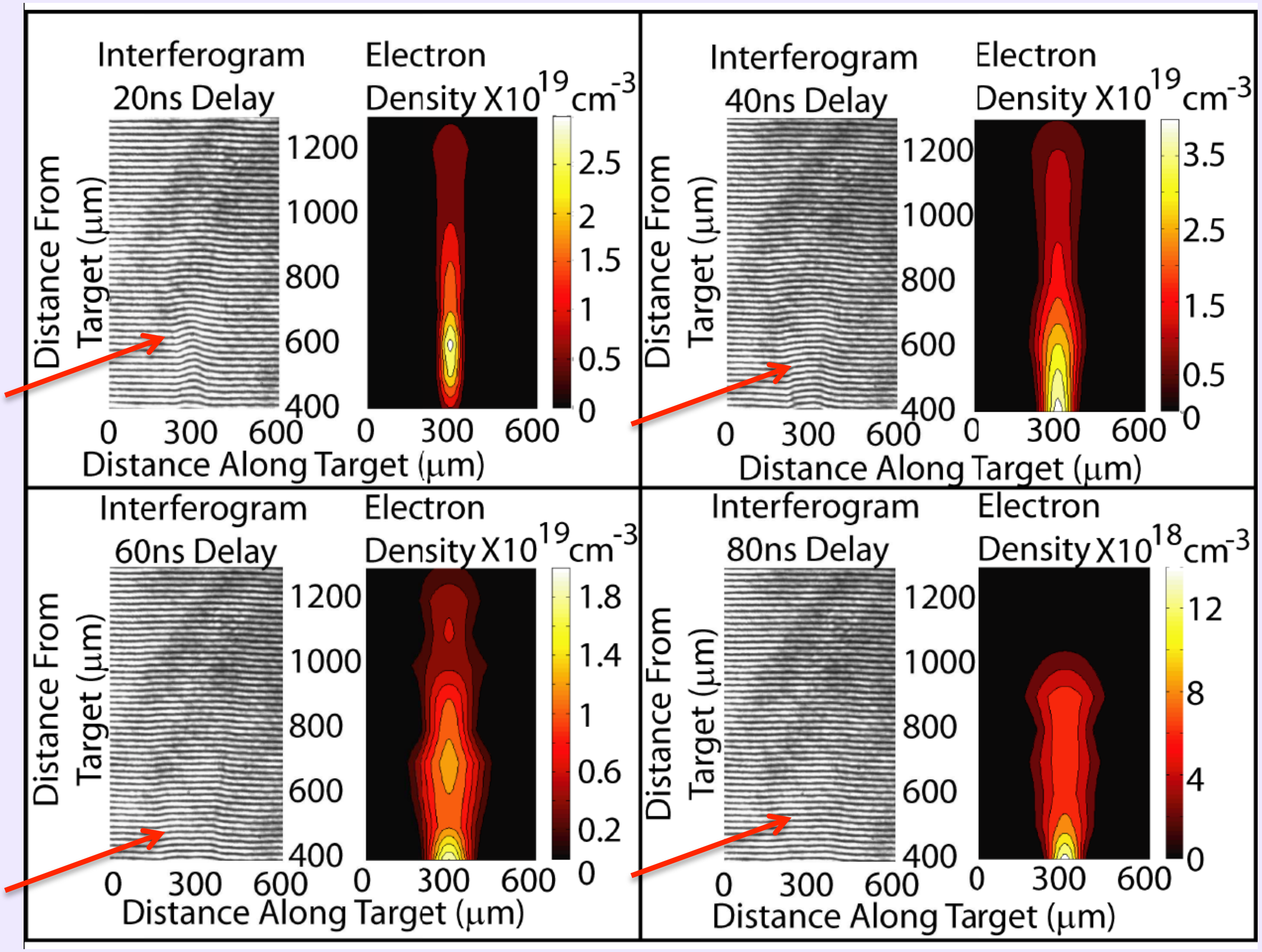

Part III – SL Diagnostics

Distinguishing electron and ion stagnation

1064 nm/ 6 ns/ 100 mJ

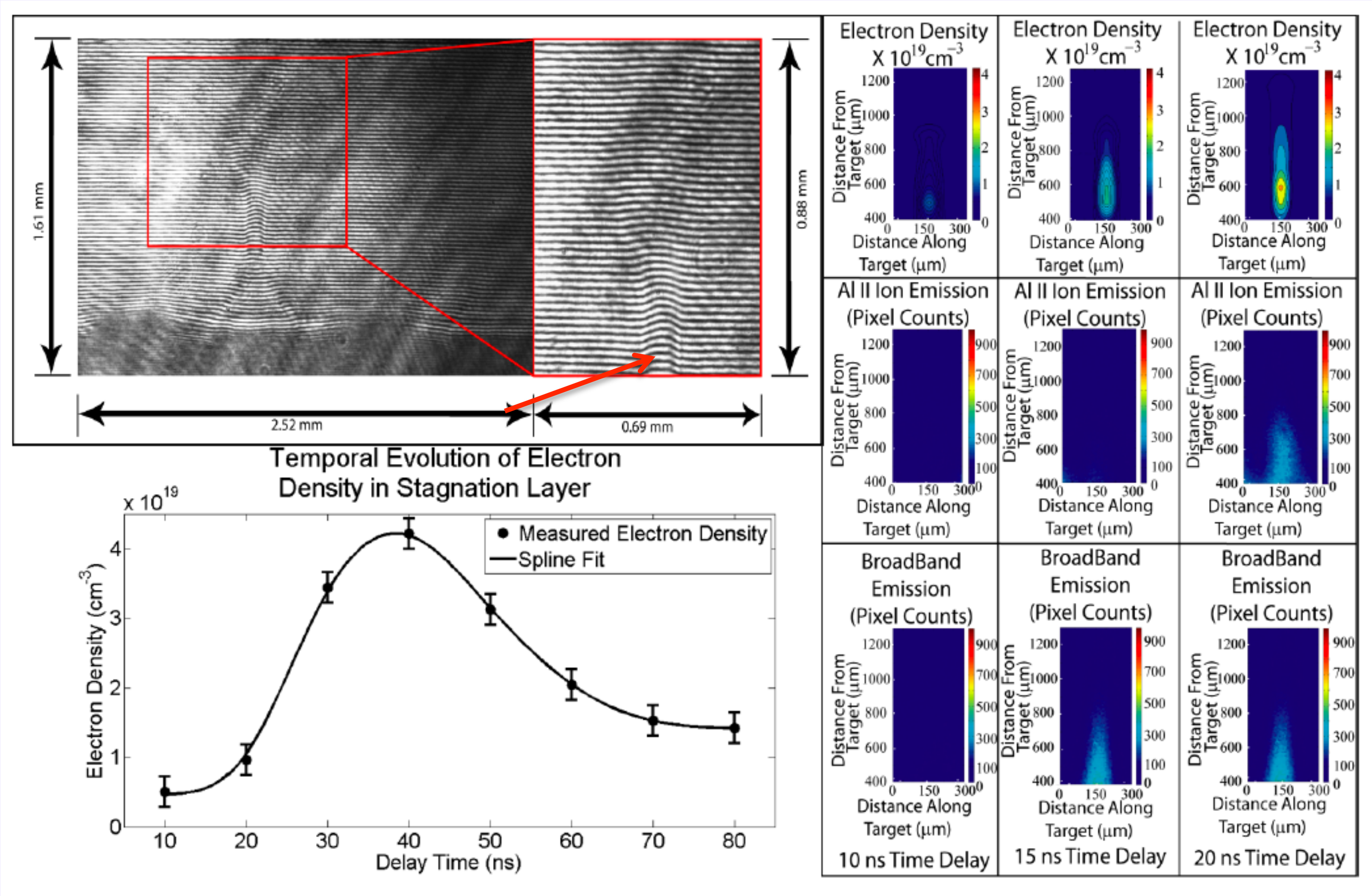

Electrons - 'Nomarski'

Al^+ ions - ICCD

Al plume - ICCD

Part III – SL Diagnostics

Motivation – colliding plasmas as **laser ion sources** - LIS

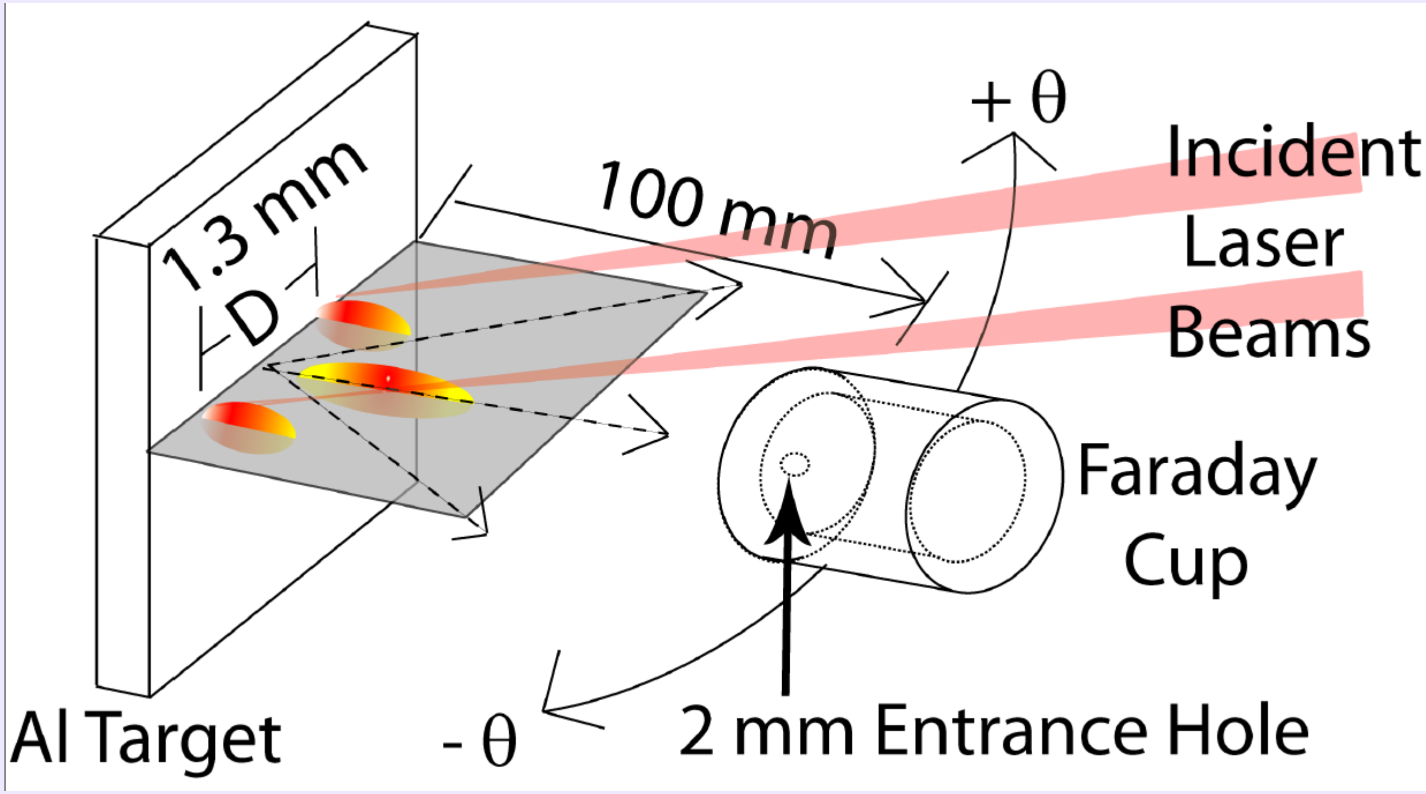

Angle Resolved Ion Emission Experiment

Part III – SL Diagnostics

Motivation – colliding plasmas as laser ion sources – ***LIS ?***

Some interest arising from potential applications in:

1. Fundamental Interactions with Particles/Fields
2. Ion implantation
3. Injector systems for ion accelerators
4. Heavy ion therapy in oncological studies

1. www.pearl2009.org
2. E Woryna et al., Rev. Sci. Instrum **72** 2 (2000)
3. B Sharkov and R Scrivens, IEEE Trans. Plasma. Phys **33** 1778 (2005)
4. A. Denker et al., NIM B **240** 61 (2005)
5. P Yeates, J T Costello and E T Kennedy, Plasma Sources Sci. Technol. **19** 065007 (2010)
6. P Yeates, J T Costello and E T Kennedy, Physics of Plasmas **17** 123115 (2010)
7. P Yeates, J T Costello and E T Kennedy, J. Phys. D: Appl. Phys. **44** 135204 (2011)

Part III – SL Diagnostics

We observe quite significant narrowing of the TOF distribution compared to single plasma plumes….!

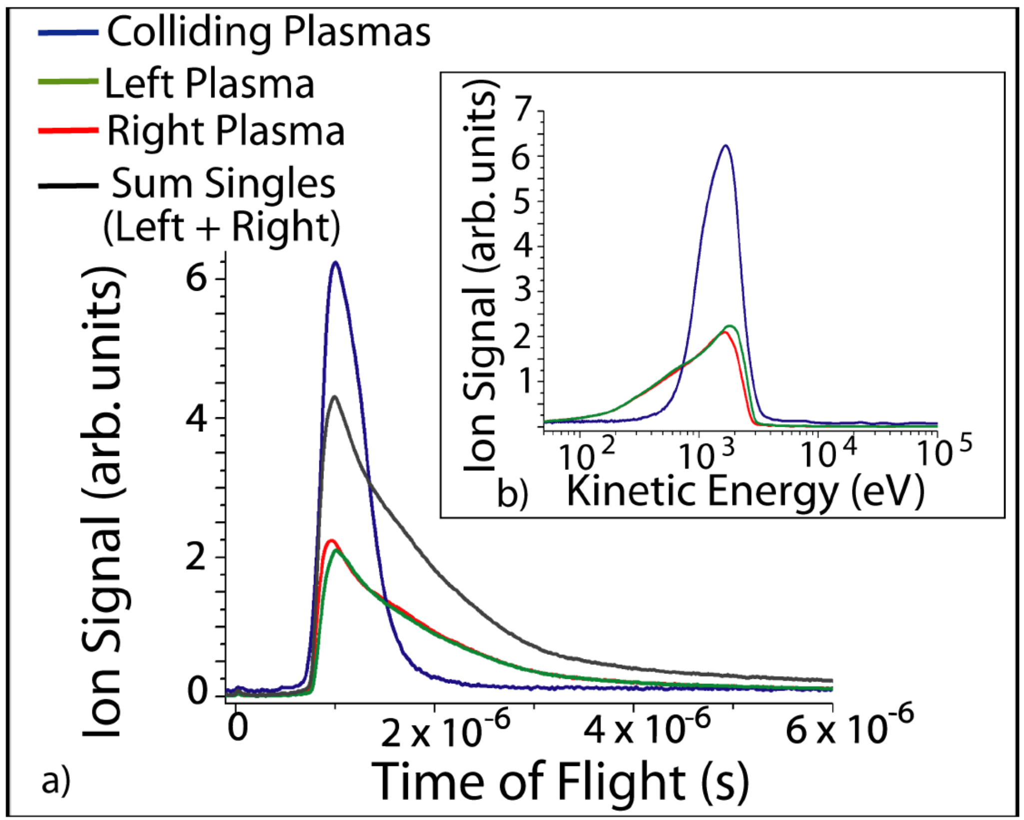

'Plasma ion bunch compression…'

P Hough, P Hayden, C Fallon, T J Kelly, C McLoughin, P Yeates, J-P Mosnier, E T Kennedy, S S Harilal and J T Costello, J. Phys. D: Appl. Phys. 44 355203 (2011)

Part III – SL Diagnostics

As we move the detector off normal emitted ion flux from each (left or right hand side) single plume dominates => weak lateral emission from stagnation layer - fewer damaging fast ions and perhaps less plasma debris ? (EUVL)

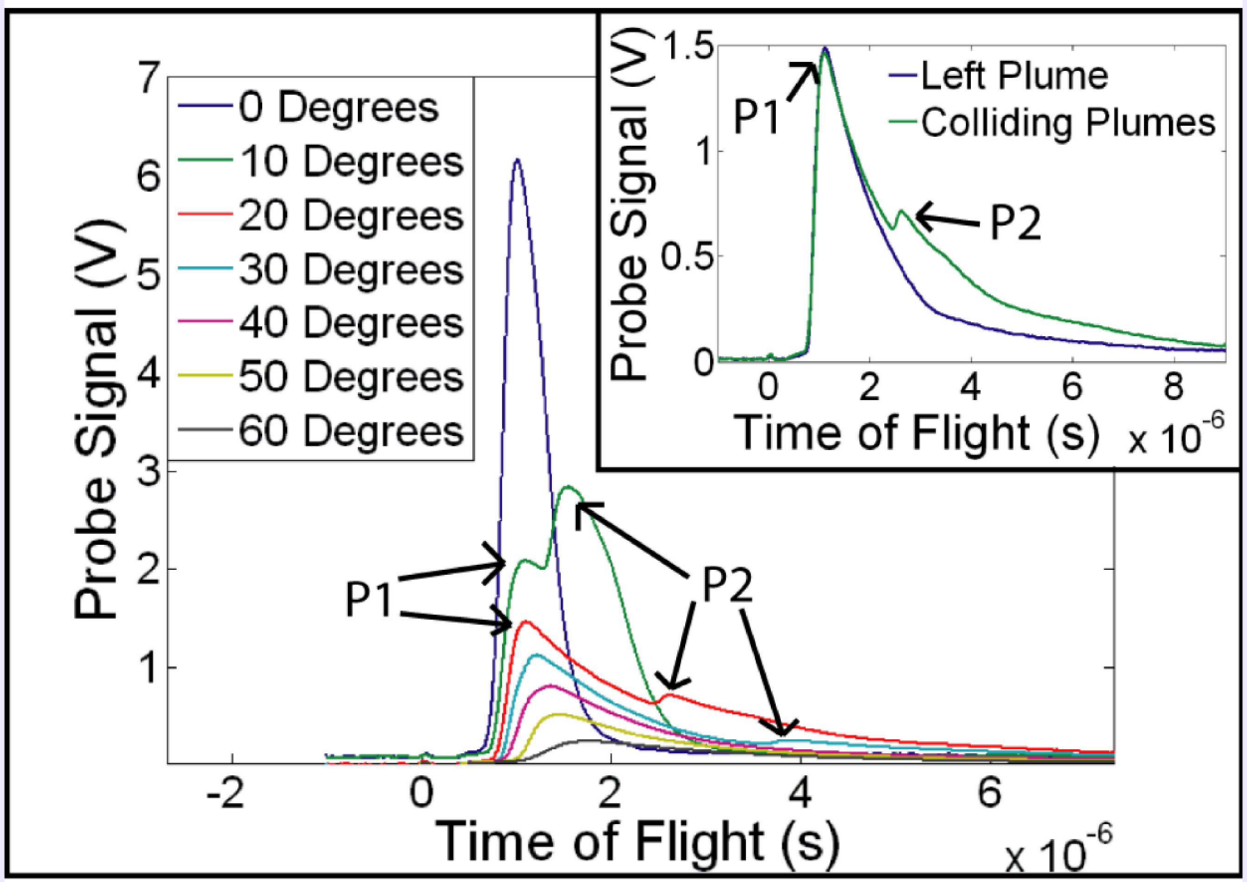

Part III – SL Diagnostics

One can also tune the width and peak energy of the 'total ion' TOF distribution with the laser energy (6ns/1064nm)

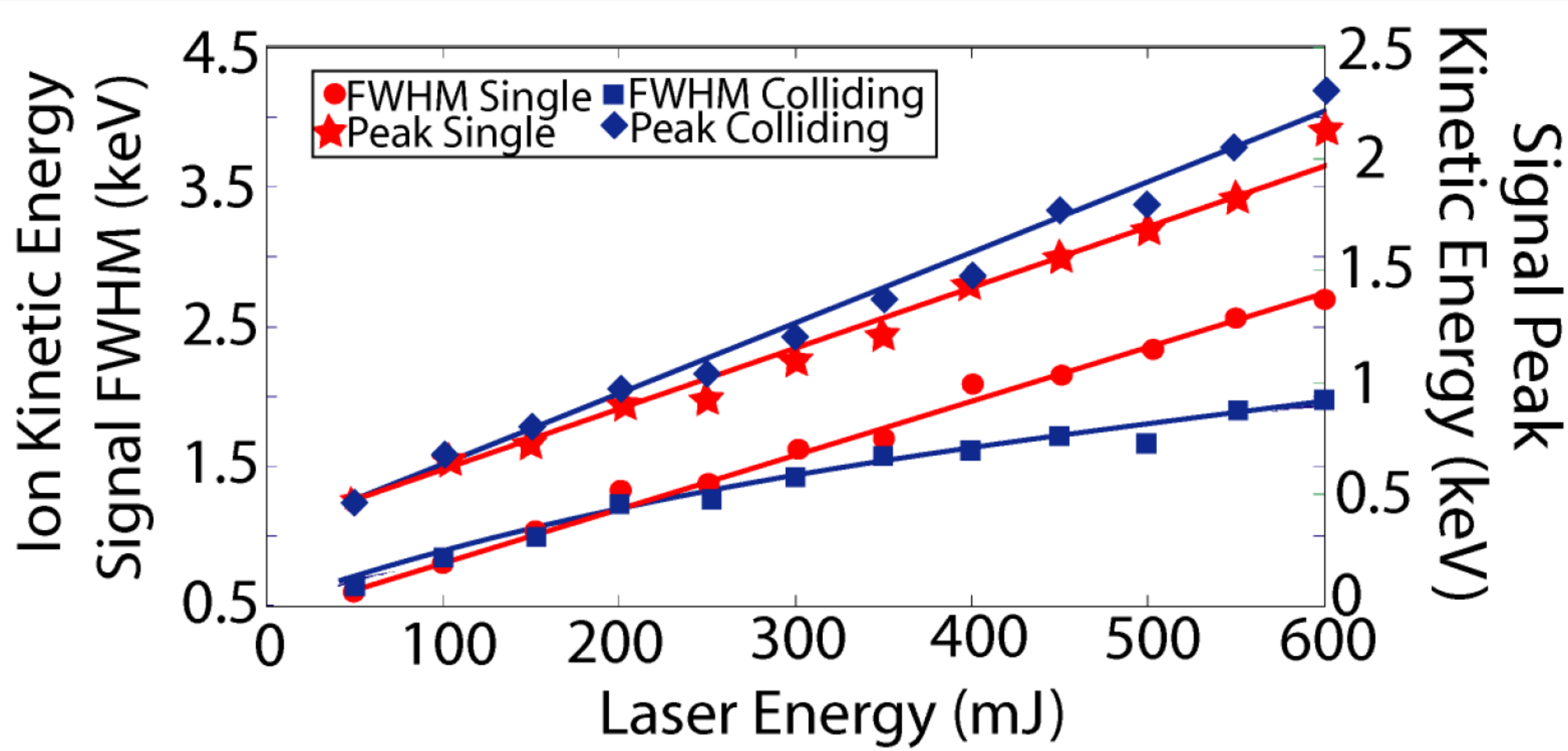

P Hough, P Hayden, C Fallon, T J Kelly, C McLoughin, P Yeates, J-P Mosnier, E T Kennedy, S S Harilal and J T Costello, J. Phys. D: Appl. Phys. 44 355203 (2011)

CP Ion Emission – Summary So Far

1. The Faraday cup entrance aperture is 2 mm in diameter and so we see all paraxial ions coming from the complete colliding plasma system.

2. Ergo the stagnation layer (stagnant field) appears to have the effect of accelerating the slow ions that are a feature of single plumes – no tail.

3. Right now we cannot say anything about the ions coming exclusively from the stagnation layer – need better spatial resolution.

4. Looks promising but much to left to do to prove potential.

Part IV. Key Properties–Potential Applications

LIBS Spectrum of ‘Coronation Rock – N165’

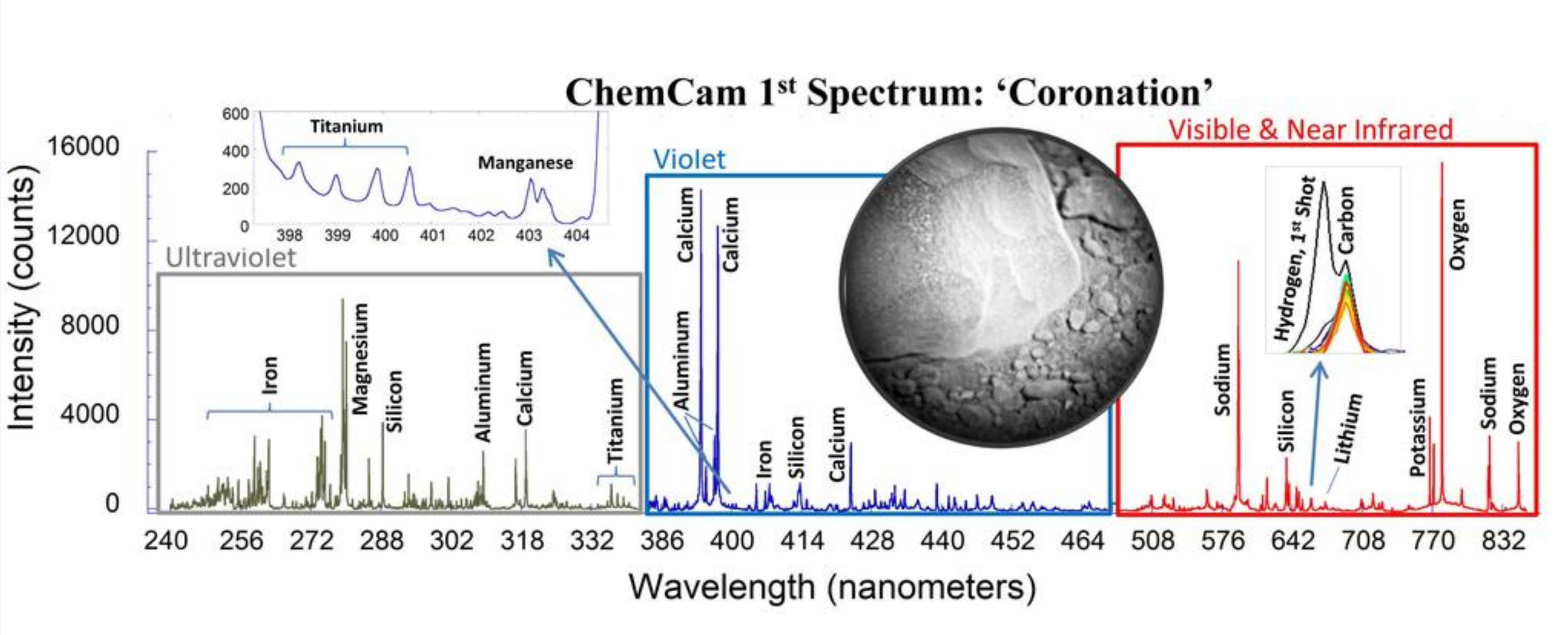

LIBS provides both classification and quantification possibilities

Received from Mars by NASA’s *Curiosity Rover* on *19th Aug 2012*
(*Picture source: http://mars.jpl.nasa.gov/msl/multimedia/images/?ImageID=4541*)

Part IV. Key Properties–Potential Applications

1. The most important of these is flexibility. Since a stagnation layer is a partially ionized plasma, it has many free parameters, which can be tuned for specific applications
2. Opacity is a problem in LIBS as radiation from the core is reabsorbed in the cooler corona - we know that the stagnation layer can be heated uniformly to reduce/eliminate opacity
3. The stagnation layer requires mainly some additional focusing optics and novel target designs and so it is easily retrofitted to existing experiments or commercial systems.
4. The emitting size of a re-heated stagnation layer can be geometrically engineered to readily match the acceptance angle of both optical and mass spectrometric systems.
5. The stagnation layer is already a pre-heated or proxy plasma for e.g., double pulse LIBS.
6. We have good preliminary evidence that we can preferentially generate high nanoparticle fluxes in nanosecond colliding plasmas
7. The position of the layer in space can be adjusted by the target geometry and relative energy in each of the seed plasma laser beams
8. It also **does not suffer from clogging** as happens in some EUVL Tin-Drop and biomolecule injector system applications
9. As we have seen stagnation layer electron densities ranging up to a few 10^{19} cm^{-3} are readily obtained while even higher densities are possible with frequency tripled Nd-YAG seed lasers.
10. We also have preliminary signs that we can control the ion energy spectrum to improve the resolution in TOF applications, reduce ion / debris damage in EUV optical systems, etc.

Part IV. Key Properties–Potential Applications

Re-excitation of SLs – towards DP LIBS

4 Wedges – 485 nm line - Sn^{2+} - time & space integrated

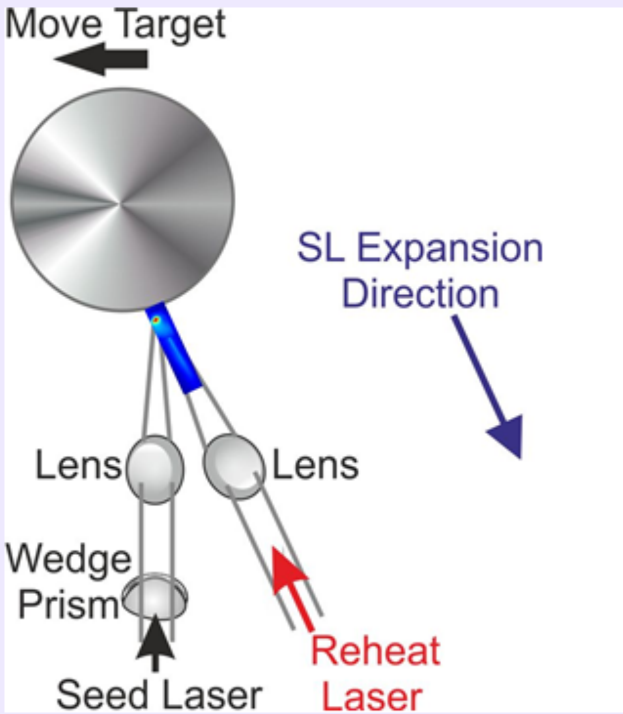

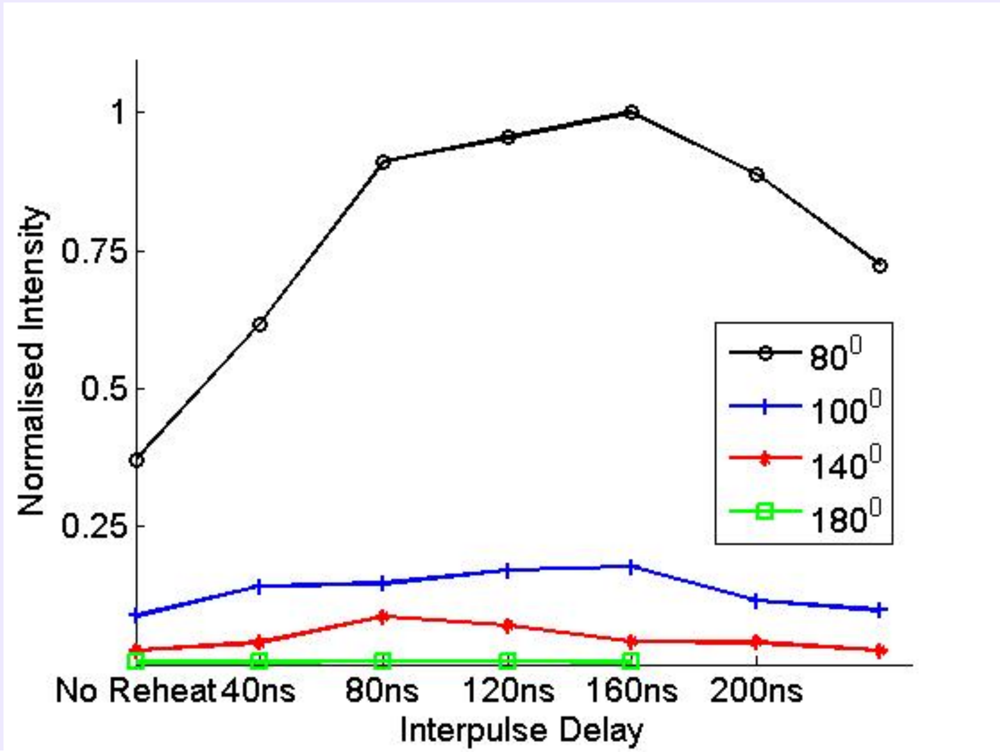

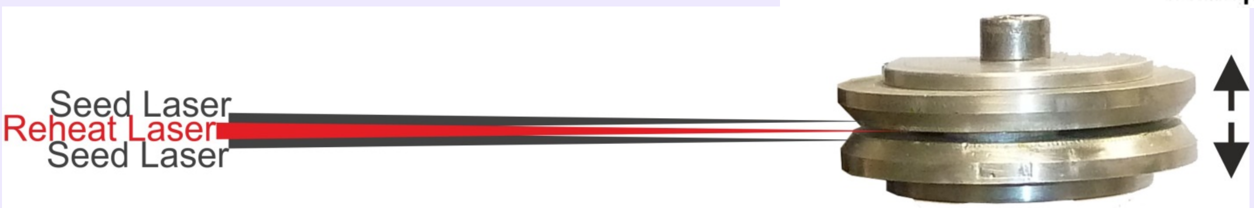

Part IV. Key Properties–Potential Applications

4 Wedges – 485 nm line - Sn^{2+} - time & space integrated

No Reheat

Inter-pulse Delay

80 ns Reheat

120 ns reheat

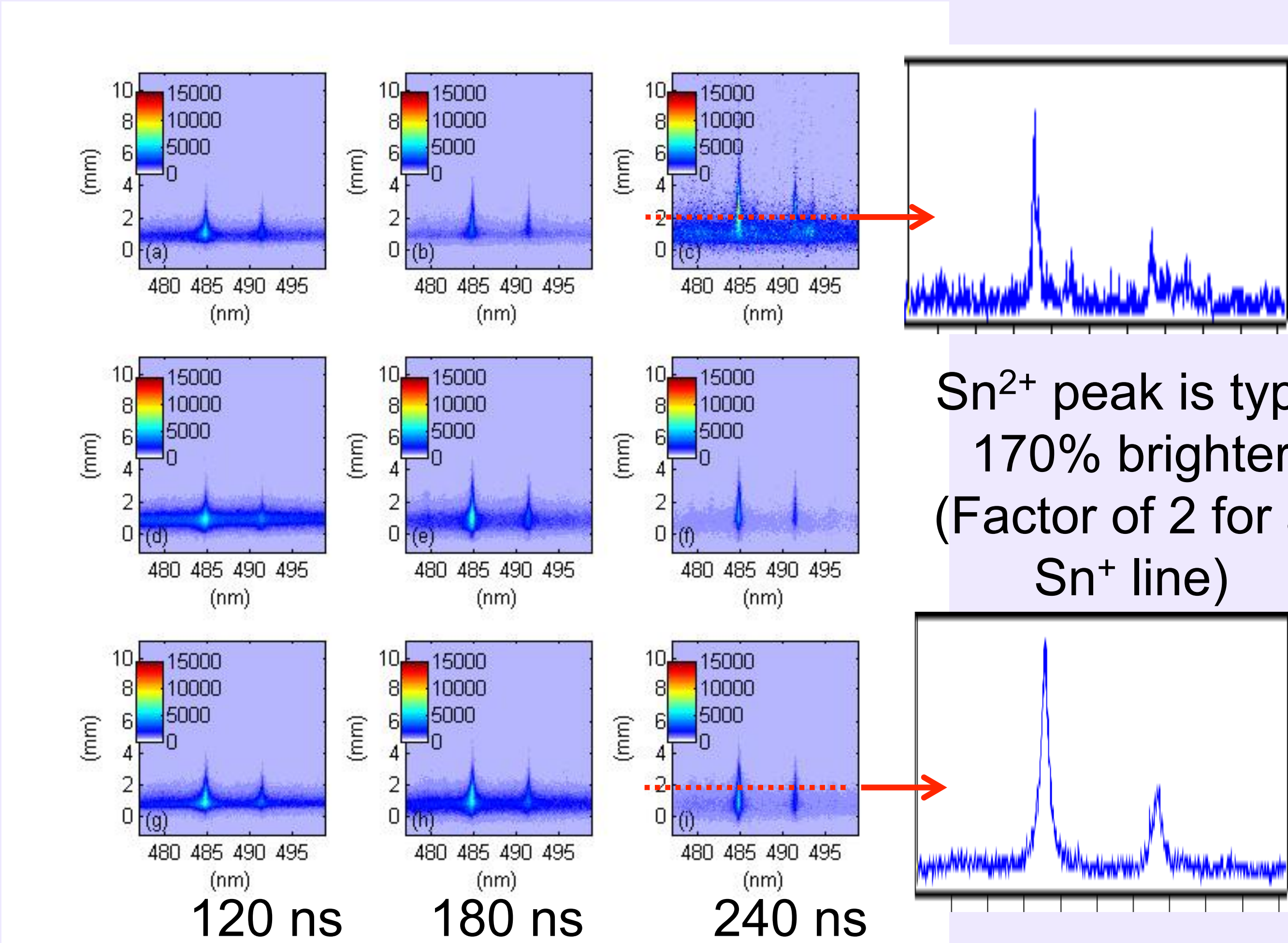

Sn^{2+} peak is typ. 170% brighter (Factor of 2 for a Sn^{+} line)

Acquisition Delay Time

Part IV. Key Properties–Potential Applications

ZnO nanoparticle Deposition – ZnO target in 10 mbar O_2

SEM IMAGES

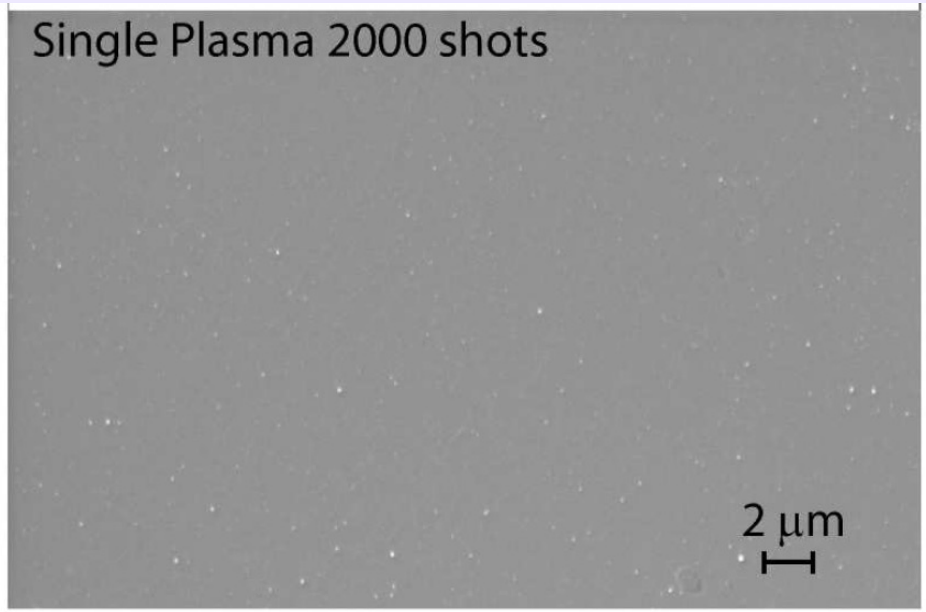

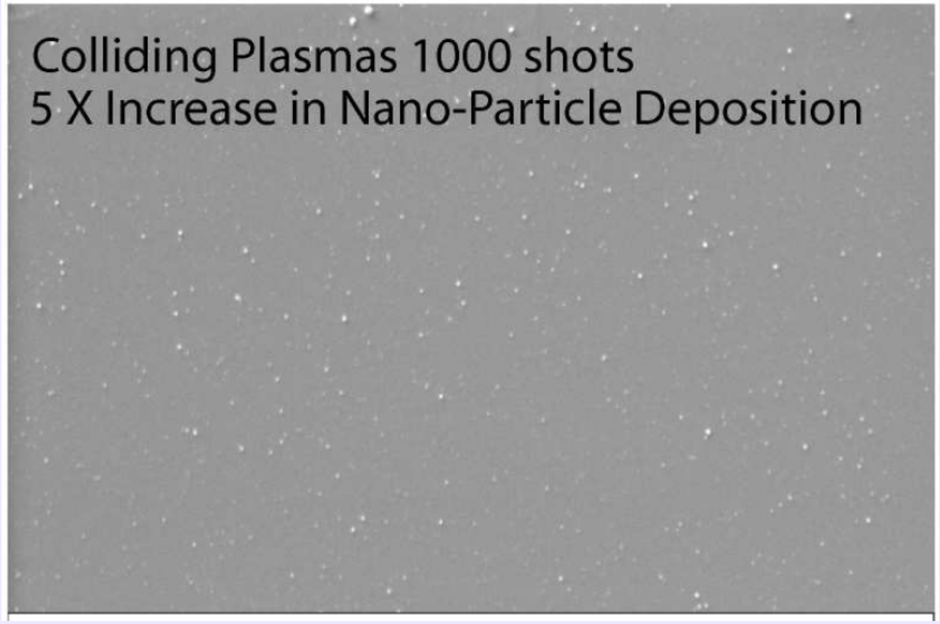

Photoluminescence of nanoparticles in vapor phase of colliding plasmas
S L Gupta, and R K Thareja, J. Appl. Phys **113** 143308 (2013)

Part V. Colliding Plasmas - Summary & Outlook

What have we learned so far - at least from the optical diagnostics ?

Part V. Conclusions – I

1. Strong stagnation in table-top colliding plasmas due to large value of the collisionality parameter (ζ)

2. Degree of confinement/hardness of the stagnation layer can be controlled by designing the value of ζ

3. Density and temperature are strongly dependent on the seed laser wavelength – so can be selected/controlled

4. Both temperature and density increase with decreasing wedge angle, *i.e. both can be controlled via target geometry*

5. We believe that more than one process determines species transport in SL

Part V. Conclusions - II

6. 'Velocities' of SL species drop as the wedge angle decreases while Ion/ neutral atom 'velocity' ratio generally >3

7. Compared to single plume the duration of self emission from atoms and ions is longer

8. Densities and temperatures remain at higher values for longer in stagnation layers

9. Stagnation layers becomes quite uniform after 100 ns

10. Ergo SLs looks attractive for investigation as an alternative pulsed laser deposition [PLD] source and for applications in laser ablation analytical sciences [LAAS]

Part V. Summary I – Next Steps

Symmetric seed plasmas….

Axicon =>
Bessel Beam + Focusing =>
Ring Plasma

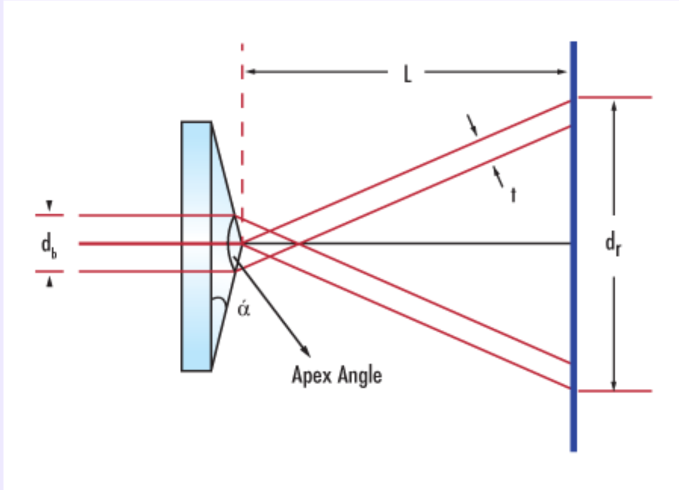

Matched Fresnel Bi-prisms
=> Symmetric Beams
+ Focusing =>
Symmetric 'Seed' Plasmas

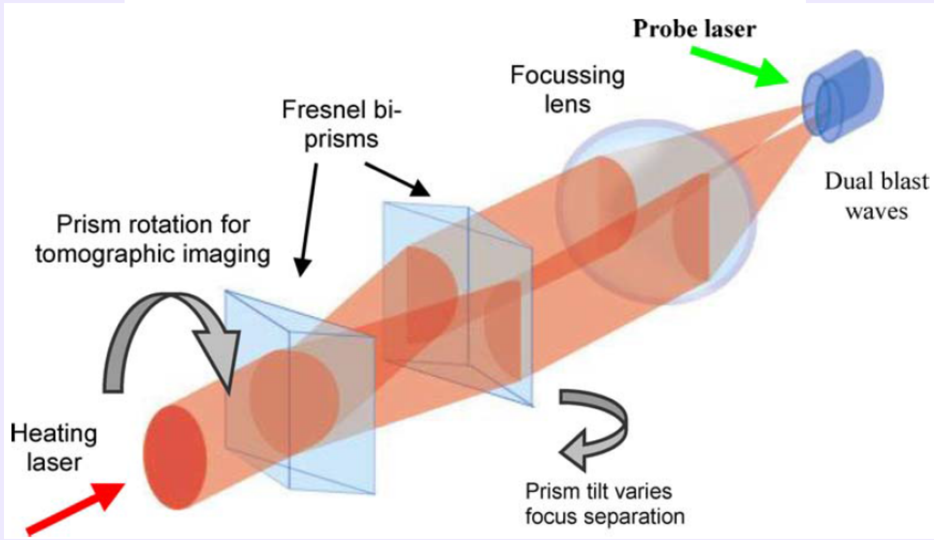

R A Smith et al., Astrophys. Space Sci. **307** pp131–137 (2007)

Part V. Summary I – Next Steps

1. Analytical Sciences: Applications of Stagnation Layers in LIBS, LAS-ICP & MALDI for LOD enhancements (NPs)

2. Bio-molecular Sciences:

Stagnation Layers as 'getters' for biomolecule aggregation in LIAD

C R Calvert, L Belshaw, M J Duffy, O Kelly, R B King, A G Smyth, T J Kelly, J T Costello, D J Timson, W A Bryan, T Kierspel, P Rice, I C E Turcu, C M Cacho, E Springate, I D Williams and J B Greenwood, Phys. Chem. Chem. Phys. **14**, 6289–6297 (2012)

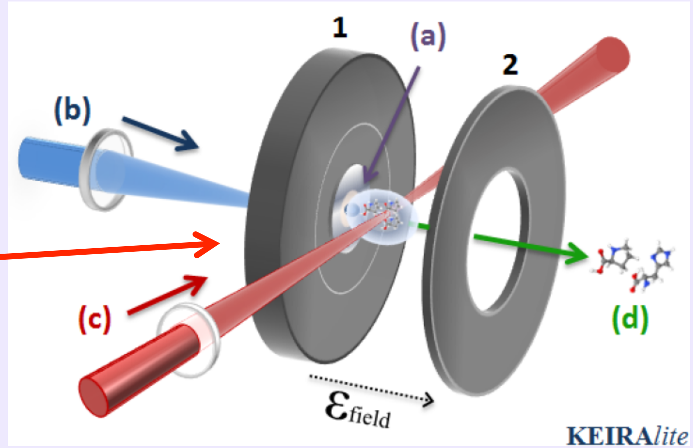

3. EUV Lithography: Stagnation Layers as self suspended targets, preheated targets (reduced opacity, ion energy narrowing, debris, etc.)

4. XUV/X-ray sources:

Applications of Stagnation Layers in double pulse experiments (especially opacity reduction in high-Z materials to enhance spectral line emission)

P K Carroll et al., Opt. Letts. **2**, 72 (1978)

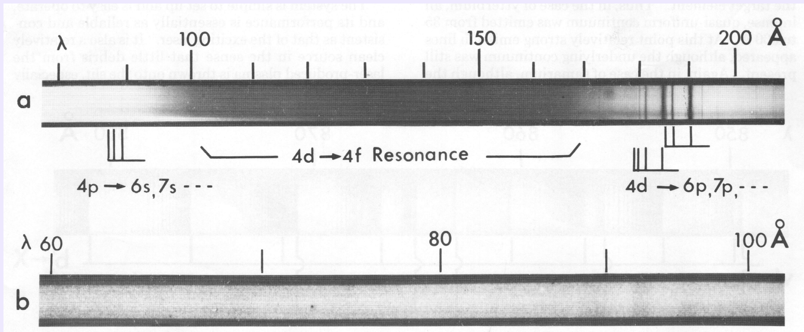

Fig. 1. (a) Absorption spectrum of xenon from 80 to 200 Å. The xenon pressure in the spectrograph was 0.05 Torr, and the number of laser pulses used was 30. For details of the xenon spectrum in this region see Madden and Codling.[5] The unmarked weak lines near 200 Å are due to 0 V. Oxygen present in the target gives rise to some emission lines as well. (b) The ytterbium continuum from 60 to 100 Å. The number of laser shots was 20. As in (a), the spectrum was obtained on a Kodak SC5 plate.

Financial Support to DCU Group

Higher Education Authority – Programme for Research in Third Level Institutes (IV and V)

Science Foundation Ireland – Investigator Prog. 12/IA/1742 & SIRG 13/SIRG/2100 (PH)

Irish Research Council (PhD Scholarships / Postdoctoral Fellowships)

EU FP7 Erasmus Mundus Joint Doctorate 'EXTATIC' – EUV and X-ray Technology and Training for Interdisciplinary Cooperation – Grant No. FPA 0033-2012